RSC Advances

REVIEW

View Article Online
View Journal | View Issue

Cite this: *RSC Adv.*, 2020, **10**, 37327

Structure and mechanical behavior of *in situ* developed Mg_2Si phase in magnesium and aluminum alloys – a review

Prem Prakash Seth, Om Parkash and Devendra Kumar *

Received 25th March 2020
Accepted 26th June 2020

DOI: 10.1039/d0ra02744h

rsc.li/rsc-advances

The demand for lightweight, high specific strength alloys has drastically increased in the last two decades. Magnesium and aluminum alloys are very suitable candidate materials. Research on alloys with an Mg_2Si phase started about three decades ago. The current scenario is that magnesium and aluminum alloys containing an Mg_2Si phase are very popular in the scientific community and extensively used in the automotive and aerospace industries. Mg_2Si is a very stable phase and exhibits excellent mechanical, thermal, electrochemical and tribological properties. This paper presents a brief review of Mg–Si binary alloys, and Mg–Si–Al and Al–Si–Mg alloys. Grain refinement methods and mechanical properties have been reported on lightweight alloys containing Mg and Si. The available results show that silicon reacts with magnesium and forms an intermetallic compound with the stoichiometric formula Mg_2Si. There is *in situ* formation of an Mg_2Si phase in Mg–Si, Mg–Si–Al and Al–Mg–Si alloys by the diffusion or precipitation process. The morphology and size of an *in situ* developed Mg_2Si phase depend on the synthesis route and base metal or matrix. In the liquid metallurgy process the precipitation sequence depends on the cooling

Department of Ceramic Engineering, Indian Institute of Technology (BHU), Varanasi 221005, India. E-mail: devendra.cer@iitbhu.ac.in

Prem Prakash Seth is Ph.D. scholar at Indian Institute of Technology (BHU) Varanasi India. His research interest includes powder metallurgy, light weight magnesium/aluminum alloys and composites, intermetallic compounds, microstructure refinement and studies of mechanical, wear and electrochemical behavior. He received B. Tech (Mechanical Engineering) from Dr A. P. J. Abdul Kalam Technical University, Lucknow (Formerly Uttar Pradesh Technical University) in 2009 and M. Tech (Steel Technology) from National Institute of Technology, Rourkela in 2014.

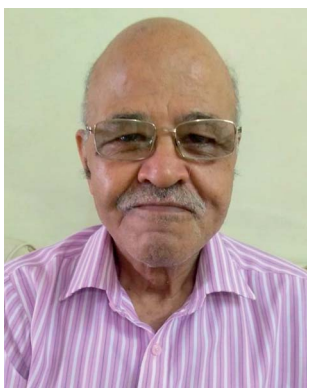

Om Parkash, a Physical Chemist and Materials Scientist (PhD from IIT Kanpur), was Professor and Head of Department of Ceramic Engineering, Indian Institute of Technology (Banaras Hindu University), Varanasi. He was a research associate in Lehigh University (U.S.A.) for one year (1988–89). During his 39 years of teaching and research career he has published more than 250 papers and guided 20 PhD and 60 M. Tech students. His research areas include electronic ceramics (electrical, dielectric and magnetic properties of rare earth transition metal oxide perovskites, varistors, glass ceramics, polymer matrix ceramic composites and dielectrics, solid electrolyte for intermediate and low temperature solid oxide fuel cells), and metal-matrix composites. He was a member of the Advisory Committees (Materials, Mining and Mineral Engineering; Physics and Mathematical Sciences for Women Scientists Scheme) of the Dept. of Science and Technology, Govt. of India for 15 years. He is a fellow of the Indian Institute of Ceramics and a life member of the Materials Research Society of India.

rate. The morphology of the Mg_2Si phase depends on the precipitation sequence and the mechanical properties depend on the morphology and size of the Mg_2Si phase within the alloy matrix.

1. Introduction

During the past quarter century, the demand for lightweight materials has drastically increased, especially for magnesium alloys and its composites. The element of magnesium is the 6th most abundant element in the earth's crust.[1] The density of magnesium (1.739 g/cc) is a minimum among different structural materials. The density of magnesium is approximately equal to two thirds that of aluminum, one fourth that of zinc, and one fifth that of iron.[2] Magnesium and its alloys possess a very high specific strength among engineering metals. Additionally, magnesium alloys show high damping capacity, excellent castability and superior machinability.[3] Currently, researchers have developed a large number of magnesium alloys. Among all these alloy systems, alloys with Mg_2Si particles are very useful. Magnesium-based Mg–Si and Mg–Si–Al alloys are primary alloys systems where Mg_2Si-phase particles are present. The Mg_2Si phase exhibits high hardness (4.5×10^9 Nm^{-2}), a high elastic modulus (120 GPa), a low density (1.99 g/cc) and a high melting temperature (1085 °C).[4] It has been reported that aluminum alloys containing an Mg_2Si phase also show better mechanical, electrochemical, and tribological properties.[5,6] Therefore, Al–Mg–Si alloys are also of great interest to the scientific community. Silicon and aluminum are the 2nd and 3rd most abundant elements in the earth's crust, respectively,[7] *i.e.* magnesium, aluminum and silicon are easily available in the earth's crust. Therefore, the cost of raw materials for Mg–Si, Mg–Si–Al and Al–Mg–Si alloys is relatively low. At ambient temperatures, these alloys can substitute for steel and copper alloys because of their better properties and lower manufacturing costs. This is the primary reason for the automobile and aerospace industry substituting denser materials with magnesium (Mg) and aluminum (Al) alloys as well as their composites.[8–10]

The mechanical properties of magnesium and aluminum alloys containing an Mg_2Si phase are primarily dependent on the average grain size, morphology, and distribution pattern of the Mg_2Si phase. The intermetallic compound Mg_2Si phase forms *via* precipitation during solidification of molten Mg–Si. After solidification, the precipitates appear in three different patterns and sizes. The patterns are needles, Chinese script and polyhedral or star-likes crystals.[11] During and after solidification the Mg_2Si phase is found in two forms: (1) coarse dendritic primary Mg_2Si and (2) Chinese script eutectic Mg_2Si. The morphologies of these Mg_2Si phases seriously worsen the mechanical properties. The primary Mg_2Si phase shows a coarse dendritic shape with sharp edges and eutectic Mg_2Si has high stress concentration at the pointed tips. Therefore, for enhancement of mechanical properties it is necessary to modify the structure of the primary and eutectic Mg_2Si phases.[11–14] Several methods have been reported for modification of the structure of an Mg_2Si phase. Superheating, directional solidification, carbon inoculation and the addition of modifiers are popular methods.[14–16] Recently Seth *et al.*[17] reported the formation of a fine Mg_2Si phase in Mg–1Si, Mg–4Si and Mg–6Si alloys *via* solid-state sintering using high-energy ball milling. Each specimen of alloy was sintered at 500 °C for 30 minutes. The microstructure of the Mg_2Si phase is completely different from that in the alloy made by the casting process. The Mg_2Si phase is irregular in shape and uniformly distributed. Kondoh *et al.*[18] synthesized Mg_2Si dispersoids *via* solid-state synthesis using a powder metallurgy process. They used fine particles of Si and the specimens were annealed at 580 °C for 240 s in a nitrogen gas atmosphere. The properties of the alloys and composites depend strongly on the physical and chemical characteristics and the microstructures of the dispersoids, *viz.* particle size, volume fraction of the dispersoids and the bonding strength between the matrix and the dispersoids. In another report Kondon *et al.*[19] reported the *in situ* formation of an Mg_2Si phase from a mixture of magnesium and silicon powder (Mg–33.33 mol% Si) by a repeated plastic working (RPW) process. During the RPW process, the *in situ* formation of an Mg_2Si phase by the reaction of magnesium and silicon is similar to the mechanical alloying process. X-ray diffraction shows that up to 150 cycles of RPW no peak of Mg_2Si was observed. On increasing the number of cycles from 150 to 600, the peak intensity of the Mg_2Si phase was enhanced. Limited literature is available for the *in situ* formation of an Mg_2Si phase *via* powder metallurgy and secondary processes. Most reports are based on the liquid metallurgy process.

The present study summarizes the results of the *in situ* formation of an Mg_2Si phase in magnesium and aluminum

Devendra Kumar is Ex. Professor and Head, Department of Ceramic Engineering, Indian Institute of Technology (Banaras Hindu University) Varanasi, India. His research areas include Electro-Ceramics (Microwave Dielectrics, Glass Ceramics Dielectrics, Varistors, Solid Oxide Fuel Cells), Bio-Ceramics, Metal Matrix Composites. Prof. Devendra Kumar has published more than 280 research articles. He has guided a large number of doctoral and masters students. He is a fellow of the Institution of Engineers and the Indian Institute of Ceramics. He is a Member of the Research Council, CSIR-Central Glass & Ceramic Research Institute, Kolkata, Chairman of the Advisory Committee, CSIR-Central Glass & Ceramic Research Institute, Kurja Centre, Khurja (U.P.) and Convener of the Flat and Coated Glass Subcommittee, CHD 10:6 of the Glass, Glassware and Laboratory Ware Sectional Committee, Bureau of Indian Standards (BIS), New Delhi.

alloys, the precipitation sequence of an Mg_2Si phase in the liquid metallurgy process, the grain refinement method, and the structure and mechanical properties of alloys.

2. Mg_2Si phase and its *in situ* development in different alloys

The *in situ* formation of an Mg_2Si phase or particles in the liquid metallurgy process *via* the precipitation of magnesium and silicon during solidification and in solid-state synthesis by diffusion of magnesium and silicon occurs according to reaction (1).

$$2Mg + Si \rightarrow Mg_2Si \quad (1)$$

Mg–Si, Mg–Si–Al, and Al–Mg–Si alloy systems are basic alloys systems, where the *in situ* developed Mg_2Si phase is present. The microstructures depend on the synthesis process and parameters. The microstructures of magnesium and aluminum alloys containing magnesium and silicon are not very homogeneous in the liquid metallurgy process during solidification, where the precipitation sequence depends on the cooling rate. The alloys synthesized *via* a solid-state method show very high homogeneity and uniform microstructures, since the Mg_2Si phase forms by a diffusion process, which depends on controlled sintering and annealing temperature and time. The microstructural homogeneity and structure–property relationships of these alloys depend on the size and amount of silicon content. Zhu *et al.*[20] reported an increase in the silicon level in Al–7.5Mg–*X*Si alloys. The degree of microstructural homogeneity increases. The improvement in microstructural homogeneity enhances the mechanical, tribological and electrochemical properties. A further description of these alloys is given in what follows.

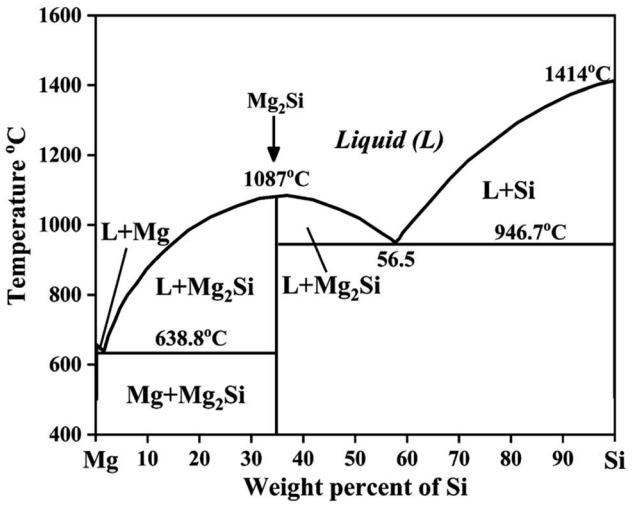

Fig. 1 Phase diagram of Mg–Si alloys. This figure has been reproduced from ref. 11 with permission from Elsevier, copyright 2008, after redrawing.

2.1 Magnesium (Mg–Si) alloys

The Mg–Si alloy system is a primary alloy system which forms an *in situ* Mg_2Si phase or particles. The maximum solid solubility of silicon in magnesium is only 0.003 at%.[17] Therefore, Si atoms react with Mg atoms, leading to the formation of the intermetallic compound Mg_2Si. Silicon improves fluidity, which allows the strengthening of Mg by precipitation hardening.[20] Therefore, the mechanical properties of Mg–Si alloys are improved. As shown in the binary phase diagram of Mg–Si in an inert atmosphere, the eutectic phase forms above 649 °C containing 1.38 at% silicon[21] (Fig. 1). Zhou *et al.*[21] synthesized the as-cast hypoeutectic Mg–1Si alloy, eutectic Mg–1.38Si alloy, and hypereutectic Mg–2Si, Mg–3Si and Mg–4Si alloys and reported optical micrographs of these alloys. The micrographs of the hypoeutectic alloy show it contains α-Mg and the eutectic Mg_2Si phase. Moreover α-Mg, the eutectic Mg_2Si phase and the beginning of the formation of a primary Mg_2Si phase appeared in the eutectic composition Mg–1.38Si. On further increasing the amount of silicon, the primary Mg_2Si phase coarsened gradually in the hypereutectic composition.

Pan *et al.*[22] studied the microstructural behavior and phase analysis of hypereutectic Mg–8Si alloy using electron probe microanalysis (EPMA) and reported that the solidification path depends on the cooling conditions. At a very low cooling rate, the solidification process is almost as per the equilibrium state. At equilibrium the solidification path is shown in eqn (2), where p represents the primary Mg_2Si particles and E represents the Mg_2Si eutectic crystals.

$$L \rightarrow L_1 + Mg_2Si_p \rightarrow Mg_2Si_p + (Mg + Mg_2Si)_E \quad (2)$$

During solidification of the liquid phase, the primary Mg_2Si precipitate initially forms in the melt. When the temperature decreases and reaches the eutectic temperature, the eutectic reaction progresses and the rest of the melt solidifies as eutectic Mg–Mg_2Si. When the solidification rate is fast, such as in the case of ingot metallurgy, then solidification is a non-equilibrium process and a different path is followed, as shown in eqn (3).

$$L \rightarrow L_1 + Mg_2Si \rightarrow L_2 + Mg_2Si_p + Mg_{sub\text{-}p} \rightarrow Mg_2Si_p + Mg_{sub\text{-}p} \rightarrow Mg_2Si_p + Mg_{sub\text{-}p} + (Mg + Mg_2Si)_E \quad (3)$$

According to eqn (3) after the formation of primary Mg_2Si particles, magnesium will subsequently precipitate as sub-primary particles (α-Mg) before the final eutectic reactions in the rest of the melt. Therefore, primary Mg_2Si particles, α-Mg and Mg–Mg_2Si eutectic crystals are present in the optical micrograph (Fig. 2(a and b)). The primary Mg_2Si dendrites show a polygonal shape with an average grain size of 30 μm.[22] Jaing *et al.*[12] reported the microstructure of the Mg–5Si alloy with an X-ray diffraction pattern. The X-ray diffraction pattern confirms the formation of the Mg_2Si phase and SEM micrographs clearly show the morphology pattern of primary Mg_2Si dendritic crystals, α-Mg halos, and a eutectic Mg_2Si structure (Fig. 2(c and d)).

Chen *et al.*[23] reported the FESEM micrographs of the primary Mg_2Si phase formed from Mg–4Si alloy. The Mg_2Si phase was an

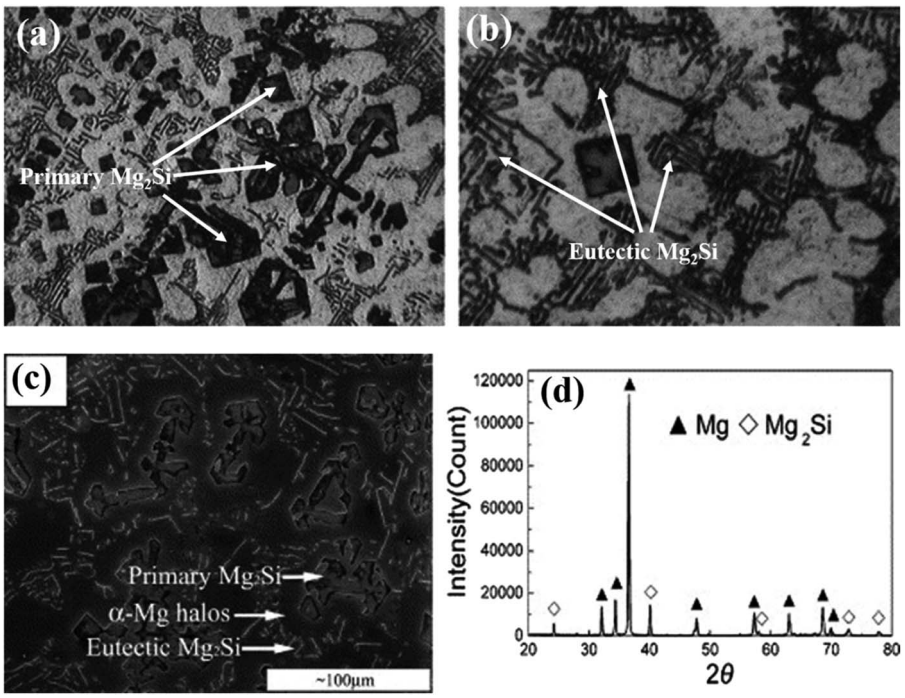

Fig. 2 (a and b) Optical micrographs of Mg–8Si alloy. These figures have been reproduced from ref. 22 with permission from Elsevier, copyright 2005. (c and d) SEM micrograph and XRD pattern of as-cast Mg–5Si alloy, respectively. These figures have been reproduced from ref. 12 with permission from Elsevier, copyright 2005.

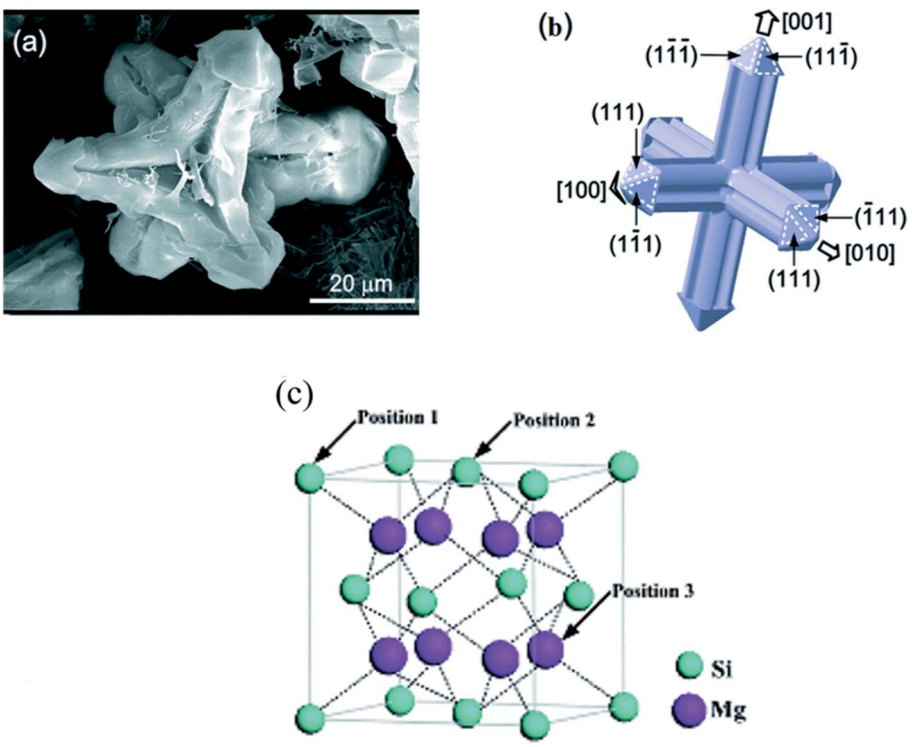

Fig. 3 (a and b) Structure and planes of the primary Mg_2Si phase. (c) Molecular structure of the Mg_2Si phase. This figure has been reproduced from ref. 23 with permission from Royal Society of Chemistry, copyright 2014.

equi-axed-dendrite with an average grain size of ~70 μm (Fig. 3(a and b)).

The crystal structure of the Mg_2Si phase is a face-centered cubic (fcc) (anti-fluorite type) with lattice parameter, a = 0.639 nm, Fig. 3(c).[23] The bonding in pure Mg_2Si is a complex kind of covalent bond. Ionic and metallic bonds are also present. The bond strength of these bonds, however, is very weak. There is only 8% ionicity in Mg_2Si. The strong covalent band of the Mg_2Si phase is dominated mainly by Si-3p and Mg-3s, 3p states. The bond strength between silicon–silicon or magnesium–magnesium atoms is very low.

The formation of the primary Mg_2Si phase is dependent on the solidification conditions.[22] The solidification begins with nucleation as well as the growth of Mg_2Si primary crystals. After nucleation, the growth will occur *via* the kinetics of atom attachment to the solid–liquid interface, heat and mass transfer, and capillarity. The growth rate of Mg_2Si dendrites is mainly solute-diffusion-controlled. Mg_2Si phase dendrites continuously grow into liquid under a high degree of super cooling, because atoms migrate rapidly towards the cooling interface. Diffusion of atoms, however, is relatively slow in the liquid. Therefore, Mg_2Si crystals show anisotropic properties, such as the interface energy, which leads to growth of dendrite arms in specific crystallographic directions, resulting in a complex dendritic morphology. The mechanical properties of these alloys are inversely proportional to the square root of the average grain size of the Mg_2Si phase. The average grain size of the Mg_2Si phase formed *via* a liquid metallurgy process (casting method) is ~100 μm.[12,24]

2.2 Magnesium (Mg–Si–Al) alloys

Magnesium (AS series) alloys containing aluminum and silicon are also very attractive for the automotive and aerospace industries due to their high potential as heat-resistant, creep-resistant and low-density materials.[25] The Mg–Si–Al (AS21) alloy was primarily developed by Volkswagen around 1970 for its stress-resistant and creep-resistant capabilities at temperatures up to 150 °C.[26] Grains of Mg–Si–Al alloys were composed of an Mg-rich solid solution (α-phase). The grain boundaries were composed of intermetallic compounds $Mg_{17}Al_{12}$ (β-phase) and a silicon-rich Mg_2Si phase.[27] The presence of the intermetallic compounds Mg_2Si and $Mg_{17}Al_{12}$ is responsible for these advantageous properties. In Mg–Si–Al alloys, Mg_2Si acts as an excellent heat-resistant strengthening phase because the Mg_2Si phase has a high melting point and a low thermal expansion coefficient.[25] During the last two decades numerous studies have been done on AS series alloys to understand their machinability and creep mechanisms at elevated temperatures.[27] AS series alloys have high creep resistance and corrosion resistance. Therefore, AS series alloys are used in automotive engine components. Zhang[28] investigated the creep behavior of the die-cast AS21 alloy at temperatures up to 150 °C under compression. Initially the creep rate (primary creep) decreases and the stress exponent n is in the range of 13–19. This is because the die-cast AS21 alloy was hardened by the stable rod-shaped Mg_2Si precipitates. Furthermore, the creep rate goes to a minimum followed by a gradual increase corresponding to work softening. The minimum value of creep rate is called secondary creep. It describes the maximum resistance to plastic deformation. The precipitation hardening by Mg_2Si rods was highly stable. During tertiary creep, work softening occurs due to the breakage of Mg_2Si precipitates. Threshold stress analysis suggests that the creep was controlled by dislocation climb and the true stress exponent could be reduced to about 5. Akyuzs[29] studied the machinability (turning test) and wear properties of AS series alloys. The turning processes were carried out *via* cross-cutting using the cutting edge of a polycrystalline diamond (TaeguTec CCGT 120408 FL K10) under dry conditions. Experimental data on cutting forces were obtained by measuring them with a strain-gauge. Akyuz[29] reported that the cutting forces increase with an increase in the Al% and cutting speed of AS magnesium alloys. The rise in the cutting forces, hardness and wear resistance in AS series magnesium alloys increases in the order AS11 < AS21 < AS41 < AS61 < and < AS91.

2.3 Aluminum (Al–Mg–Si) alloys

Similarly, aluminum alloys containing Mg and Si are heavily used in engineering applications[30] for critical structural shapes because these alloys have super ductility with high strength.[31] The 6XXX series[32] of alloys are mainly Al–Mg–Si alloys. Moreover, the 3XX.0 series, the 4XX.0 series of cast alloys and the 4XXX series of wrought alloys may also be Al–Mg–Si alloys. The characteristics of the 6XXX series of alloys are heat treatability, high corrosion resistance and excellent extrudability. The mechanical properties of these alloys can be easily improved by conventional thermo-mechanical processing, including quenching, cold drawing, and artificial aging.[33] The required level of mechanical strength can be achieved through dislocation strengthening and precipitation hardening. Enhanced electrical conductivity is attained by a decrease in the content of solute Mg and Si atoms in the Al matrix. In the 3XX.0, 4XX.0 and 4XXX series of alloys, magnesium is intentionally added to induce precipitation hardening *via* the formation of an Mg_2Si phase, metastable phases, or Guinier–Preston zones.[34] During the last two decades a lot of research has been done on Al–Si–Mg alloys. Generally, the precipitation behavior of Al–Mg–Si alloys is considered to follow the sequence shown in eqn (4).

$$\text{Supersaturated solid solution (SSSS)} \rightarrow \text{Cluster/GP zones} \rightarrow \text{metastable } (\beta'') \rightarrow \text{metastable } (\beta') \rightarrow \text{stable } (\beta) \text{ (ref. 35)} \quad (4)$$

The addition of an excess amount of silicon in Al–Mg–Si alloys significantly promotes the precipitation of silicon, forming fine precipitates with an unknown structure. The excess Si is tied up with the clusters/zones and β″ particles. The β″ particles are rapidly dissolved during high-temperature heating or aging and Si and other precipitates are formed.[36] Mandal *et al.*[37] reported that hypereutectic Al–Si–Mg alloys with more than 2 wt% Mg exhibit a microstructure in which the Si particles are inherently refined and uniformly distributed. On further increasing the Mg content, both the amount and size of the Mg_2Si phase increase. It has been reported that during isothermal aging (in the temperature range 150 °C to 200 °C), the strength of Mg–Si–Al alloys increases rapidly.[38] With the high rate of cooling of Mg–Si–Al

alloys, supersaturated solids are formed. With the help of isothermal aging or the age hardening process, the supersaturated solid solutions are transformed and very fine coherent or semi-coherent precipitates nucleate and grow.[38]

For a better understanding of magnesium and aluminum alloy systems containing an Mg_2Si phase, it is necessary to study the refinement modification method. Because of refinement, the morphology and grain size are primarily responsible for the enhancement in mechanical properties.

3. Synthesis routes of the formation of *in situ* Mg_2Si phase

The synthesis processes of magnesium and aluminum alloys containing an Mg_2Si phase are approximately similar. Generally, liquid metallurgy, powder metallurgy and mechanical alloying methods are used for the *in situ* fabrication of alloys containing an Mg_2Si phase. Each synthesis process uses a controlled atmosphere. The formation of the Mg_2Si phase occurs *via* the precipitation or diffusion of silicon into magnesium. Apart from liquid metallurgy, powder metallurgy and mechanical alloying, a few novel methods have also been reported by researchers: *e.g.* mechanically recitative extrusion process and spark plasma sintering.

3.1 Liquid metallurgy process

In the liquid metallurgy process, the alloying elements (powder or ingot forms) and base metal (magnesium or aluminum) are heated at high temperature, in an inert gas atmosphere. When the metal has melted, the liquid metal is poured into a mold, within which it solidifies into the required shape. At high temperature magnesium has high affinity towards oxygen. Therefore, the fabrication of magnesium alloys and aluminum alloys containing magnesium is very challenging. To overcome the limitations of the conventional casting process, various new techniques have been developed for the casting of magnesium-based alloys. High-pressure die casting, gravity casting (permanent mold casting and gravity sand casting) and other relevant casting processes, *e.g.* squeeze casting, thixo-casting and thixo-molding, are used to produce lightweight high-performance aerospace, automotive and defense equipment components.[39,40] Kumar *et al.*[5] synthesized hypo (Mg–0.5, 0.7, 1.15 wt% Si) and hyper (Mg–2, 4, 6, 8 and 10 wt% Si) eutectic Mg–Si alloys using the gravity casting method and reported that the wear rate of Mg–Si alloys decreases with an increase in Si addition under normal loads. Dargusch *et al.*[41] synthesized Mg–Si–Al alloys *via* high-pressure die casting and reported that the morphology of the Mg_2Si phase is a function of silicon content. Similarly Dwivedi *et al.*[42] reported the influence of silicon content (varying from 4 to 20 wt%) on the mechanical properties of cast Al–Si–Mg alloys. Ductility reduced monotonically and hardness increased with increasing silicon content over the range 4–20%. Generally, casting processes are economical fabrication techniques.[43,44]

3.2 Powder metallurgy process

In general, powder metallurgy includes the mixing of powders, pressing, degassing and sintering under a controlled atmosphere or in a vacuum. Generally, powders have particle sizes less than 1000 nm. Powder particles have a high ratio of surface area to volume. This helps the use of metal powders as catalysts in various metallurgical and chemical reactions.[45] The metal powders are consolidated *via* three basic approaches: (1) pressure-based densification, (2) sinter-based densification and (3) hybrid densification. Pressure-based densification establishes density *via* the compaction pressure, the surface energy of the powder particles and sintering parameters. This process is mainly used by researchers and industry. The powder particles have irregularities, good flow characteristics and must be compressible. The compacted specimens of these particles show high green density (density before sintering). Irregular particles have a high surface energy and the powder has the ability to withstand higher compressibility during compaction. These particles are highly plastically deformed and easily interlocked. Seth *et al.*[17] reported the SEM micrographs of pure

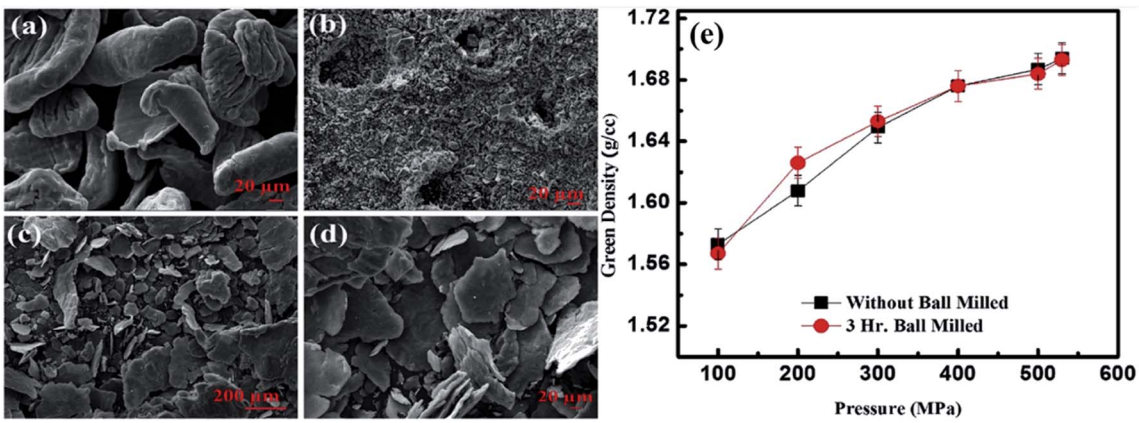

Fig. 4 SEM micrographs of (a) pure magnesium powders, (b) silicon powders, (c and d) Mg–Si alloy powders at two different magnifications and (e) the green density of pure magnesium powders with and without ball milling and compacted at different pressures. This figure has been reproduced from ref. 17 with permission from Elsevier, copyright 2020.

magnesium, silicon (as received) and magnesium–silicon alloy powder after three hours of ball milling and reported the effect of compaction pressure on the green density of magnesium powder with and without ball milling at different compaction pressures.

Fig. 4(a–d) show the SEM micrographs of magnesium, silicon and magnesium–silicon alloy powders at two different magnifications. The morphologies of magnesium and silicon are irregular semi-elliptical three-dimensional structures and irregular angular fine as well as coarse crystal shapes, respectively (Fig. 4(a and b)). The morphologies of the alloy powders after three hours of ball milling are shown in Fig. 4(c and d). Magnesium particles were converted into irregular thin sheets like lamellae. The size of the silicon particles was reduced without any change in the morphology.

Fig. 4(e) shows the green density of as-received and 3 hours-ball-milled powders. The green density of both as-received and ball-milled powders increased rapidly with an increase in the compaction pressure up to 300 MPa. However, the rate of increase of green density diminishes with increasing load after a load of 300 MPa in both cases. Moreover, the green density of as-received powder and 3 hours-ball-milled powders are same at a higher compaction pressure (400 MPa to 530 MPa). The green density at a pressure of 530 MPa is >95% of the theoretical density of pure magnesium. Therefore, researchers generally use a pressure-based densification process for the fabrication of Mg–Si alloys and composites.

The second process of powder metallurgy was sintering-based densification. In sintering-based densification the molding process is used to give the shape of the components. Generally, metal powders are mixed with binder (wax and plasticizers) and the mixture is poured into a molding machine (a metal injection molding machine). Green specimens are received from the molding machine. Before sintering, the binders are removed by a debinding process. The densification is enhanced by using finer powder particles and a higher sintering temperature. Scharrer *et al.*[46] fabricated the AZ, AJ and AS series of alloys *via* the magnesium injection molding process and reported the yield strength of the AS41 alloy.

The third process of powder metallurgy is hybrid densification. In the hybrid-densification process, pressure and temperature are applied at the same time. Spark sintering and hot pressing (often in an inert atmosphere or vacuum) are hybrid-densification processes. Sun *et al.*[47] synthesized Mg–Mg_2Si composites *via* the solid-state reaction of magnesium and silicon by using spark plasma sintering (SPS) techniques. The reaction occurs by diffusion of magnesium and silicon, leading to the formation of an Mg_2Si phase. The activation energy of formation of the Mg_2Si phase was found to be 376.0 kJ mol^{-1}.

3.3 Mechanical alloying

Mechanical alloying (MA) is the other powder metallurgy process used to develop intermetallic compounds in metals powders. MA is a solid-state synthesis technique that involves repeated fracturing and re-welding of powder particles in a high-energy ball mill. This technique is also used to synthesize supersaturated solid solutions, intermediate phases, quasi-crystalline phases, amorphous alloys, and high-entropy alloys.[48] This technique is also used to produce very fine crystallite sizes down to the nano-scale.[49] There are very few published reports concerning the formation of an Mg_2Si phase by mechanical alloying at present. Niu *et al.*[48] formed the Mg_2Si phase *via* a mechanical alloying method using a high-energy planetary ball mill. Stoichiometric compositions of magnesium and silicon powders are milled at 250 RPM with a ball to powder ratio of 20 : 1 for 30 hours. X-ray diffraction patterns are taken after 0, 6, 10, 20, 30 hours of ball milling. X-ray diffraction patterns of the ball-milled powders show that the peaks of the Mg_2Si phase are initially seen in powders ball milled for 10 hours. The relative intensity of the Mg_2Si phase peaks increased with an increase in the ball milling time. This indicates that a longer milling time leads to the formation of more Mg_2Si phase. The activation energy for the formation of the Mg_2Si phase is found to be 215 kJ mol^{-1} based on the Kissinger approach. Similarly, Jung *et al.*[50] successfully synthesized thermoelectric Mg_2Si by a mechanical alloying method for 24 hours of ball milling and examined the electronic transport properties (Hall coefficient, carrier concentration and mobility) and the thermoelectric properties (Seebeck coefficient, electrical conductivity and thermal conductivity). Mg_2Si shows n-type conduction behavior. This indicates that the electrons are responsible for the electrical conduction.

3.4 Other process

Liquid metallurgy, powder metallurgy and mechanical alloy processes are suitable and highly acceptable methods for the *in situ* development of Mg_2Si for the scientific community. Some reports show that an *in situ* Mg_2Si phase is developed *via* a repetitive extrusion or mechanical working process. The mechanism of development of the Mg_2Si phase *via* mechanical working and extrusion processes can be diffusion controlled similar to power metallurgy and mechanical alloying. Aizawa *et al.*[51] reported a mechanically induced reaction for the solid-state synthesis of Mg_2Si. In general, the mechanically induced reaction occurs *via* two processes: a nucleation controlled

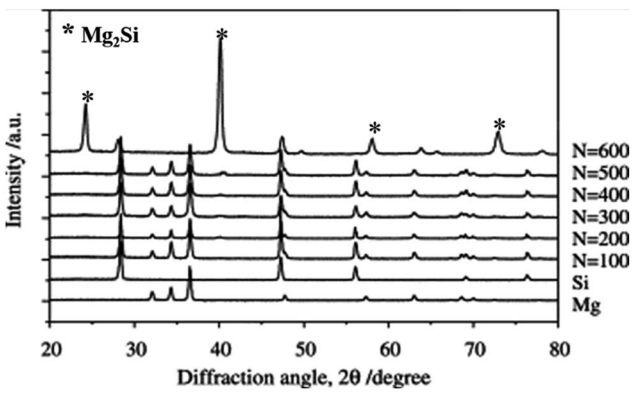

Fig. 5 Variation in XRD profiles with increasing number of cycles in the bulk mechanical alloying for the Mg–Si system. This figure has been reproduced from ref. 51 with permission from Elsevier, copyright 2006.

process with a fast reaction rate and a diffusion-controlled process with a sluggish reaction rate. For the mechanically induced reaction, bulk mechanical alloying (BMA) is used. The BMA depends on the severe plastic flow of constituents prior to the solid-state reaction at room temperature. The BMA method is applicable when the starting materials are granules or platelet forms of the order of millimeters. The pass schedule with the BMA process, one forward extrusion and two compression modes, was employed for each cyclic loading. A stoichiometric composition of magnesium and silicon powder is used for the synthesis of the Mg_2Si phase. Fig. 5 shows the X-ray diffraction pattern of Mg–Si compacts after 100, 200, 300, 400, 500, and 600 BMA cycles. The pattern shows that the formation of the Mg_2Si phase is initiated after 500 cycles.

4. Mg_2Si phase refinement methods

An enormous number of techniques have been reported to refine the microstructures of magnesium and aluminum alloys. The present work is only concerned with the refinement of those aluminum and magnesium alloys which have an *in situ*-developed Mg_2Si phase. The refinement leads to a homogenous microstructure which reduces segregation and pore formation. This enhances the mechanical and electrochemical properties.[52] A few review articles are also available for the grain refinement of magnesium and aluminum alloys. To the best of our knowledge, no review article is available on the topic of refinement in magnesium and aluminum alloys with an *in situ*-formed Mg_2Si phase.

4.1 Refinement *via* addition of modifier

The addition of a modifier is one of the most popular methods for refining the Mg_2Si phase. Yttrium, lanthanum, bismuth, cerium, KBF_4 *etc.* are used as modifiers for structural modification of the Mg_2Si phase. These modifiers are divided into three groups: (I) group one is where the modifying elements work as heterogeneous nucleation sites because of two-dimensional misfit. The Bramfitt theory shows that if the mismatch between two planes is not more than 15%, then one phase can work as the heterogeneous nucleation site for another. (II) Group two is where modifying elements decrease the onset crystallization temperature and increase the undercooling degree. Classic solidification theory, the morphological modification of the Mg_2Si phase *via* the addition of modifying elements, can be investigated based on the following two aspects. First, intermetallic compounds formed from the alloying elements act as heterogeneous nucleation sites on the liquid/solid interface because of the difference in the distribution coefficient (k). Second, increasing the degree of undercooling decreases the size of the critical nucleus radius. In this respect, heterogeneous nucleation is facilitated by the reduced size of the critical nucleus radius. (III) Group three is where modifying elements reduce the surface energy of Mg_2Si crystals by lattice distortion because of the presence of solutes.[53] The presence of modifying elements at the liquid–solid interface could restrict the growth of an Mg_2Si phase. Because these elements can be adsorbed in Mg_2Si, the surface energy of Mg_2Si is reduced by lattice distortion.

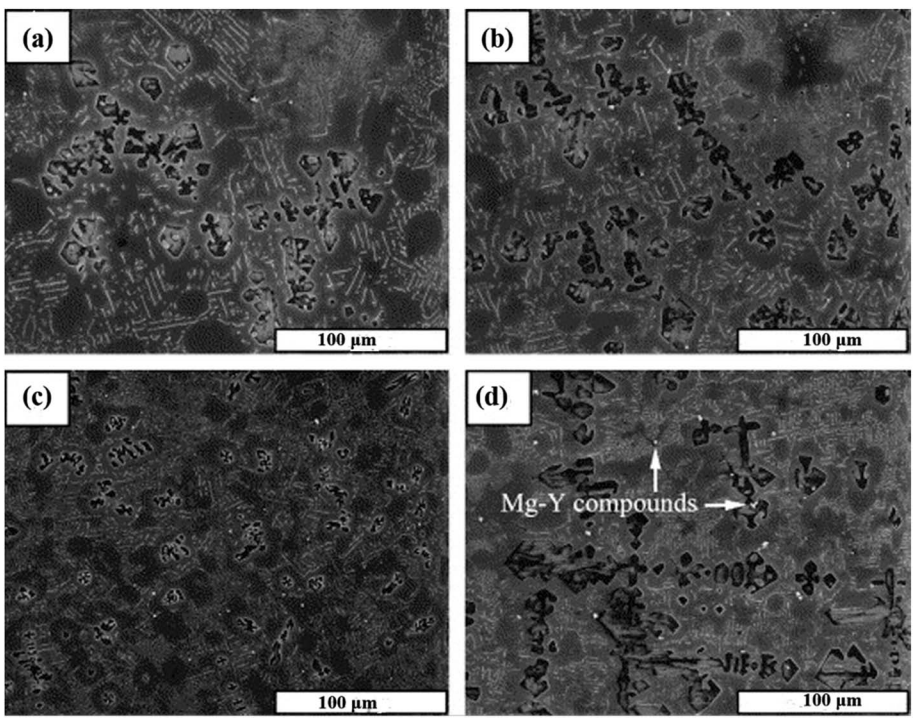

Fig. 6 SEM micrographs of Mg–5 wt% Si alloy with (a) 0.1 wt%, (b) 0.4 wt%, (c) 0.8 wt% and (d) 1.2 wt% of Y addition. This figure has been reproduced from ref. 12 with permission from Elsevier, copyright 2005.

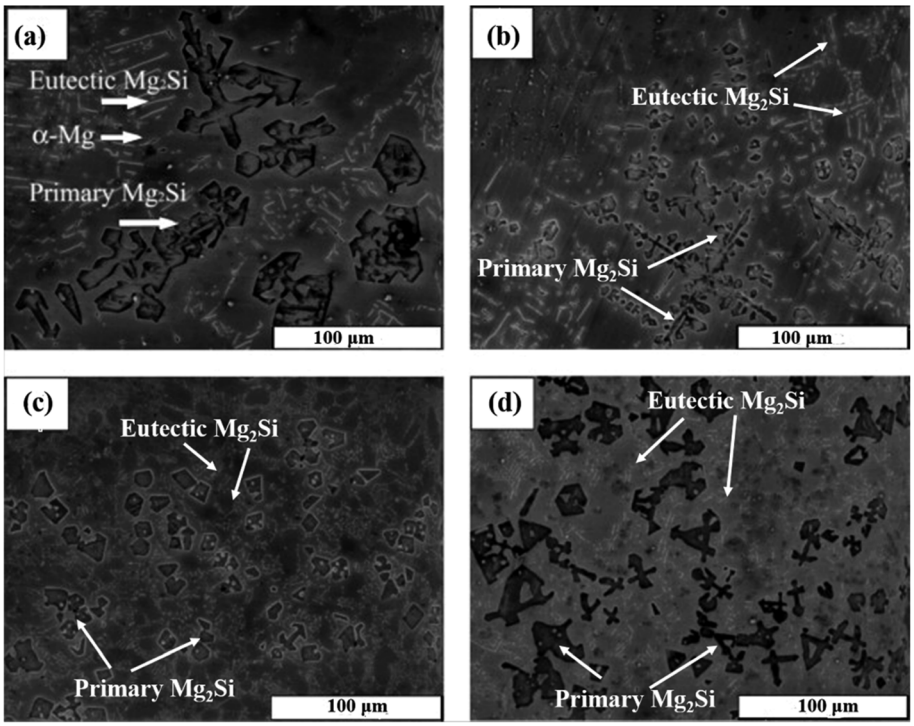

Fig. 7 SEM micrographs of Mg–5 wt% Si alloys (a) without modifier, (b) 5 wt% K_2TiF_6, (c) 5 wt% KBF_4 and (d) 5 wt% KBF_4 + K_2TiF_6 (mixtures with weight ratio of 4 : 1). This figure has been reproduced from ref. 24 with permission from Elsevier, copyright 2005.

Table 1 Effect of K_2TiF_6, KBF_4 and KBF_4 + K_2TiF_6 in Mg–5Si alloys.[24]

Modifiers	Effect of modifier	Morphology
K_2TiF_6 (5 wt%)	The size of primary and eutectic Mg_2Si phase particles are slightly reduced	Primary Mg_2Si – dendritic shape Eutectic Mg_2Si – Chinese script
KBF_4 (5 wt%)	Average grain size of primary Mg_2Si phase significantly decreased from 100 μm to ~20 μm	Primary Mg_2Si – polyhedral shape Eutectic Mg_2Si – fine fibers
KBF_4 + K_2TiF_6 (5 wt%) weight ratio 4 : 1	Primary Mg_2Si became coarser, and eutectic Mg_2Si became finer	Primary Mg_2Si – irregular shape Eutectic Mg_2Si – modified morphology with a finer size

Jiang *et al.*[12] modified the Mg–5 wt% Si alloy by the addition of 0.1, 0.4, 0.8 and 1.2 wt% of yttrium (Y). At an early stage of solidification, the addition of a small amount of yttrium forms Y-containing compounds in magnesium–silicon melts, because Y has a relatively high solubility in magnesium alloys. Y-containing compounds act as heterogeneous nucleation sites

Table 2 Effect of modifiers on average grain size of the Mg_2Si phase in magnesium and aluminum alloys

		Results	
Alloy phase composition	Modifiers	Average grain size of primary Mg_2Si grains in unmodified alloys	Minimum size of primary Mg_2Si grain in modified alloys
Mg + 5Si/Mg–Si^{12}	Yttrium	~100 μm	~30 μm at (0.8 wt% of yttrium)
Mg + 5Si/Mg–Si^{14}	Lanthanum	~100 μm	~25 μm at (0.5 wt% of lanthanum)
Mg + 5Si/Mg–Si^{11}	Bismuth	~100 μm	~15 μm at (0.5 wt% of bismuth)
Mg + 5Si/Mg–Si^{13}	KBF_4	~90 μm	~20 μm at (2–10 wt% of KBF_4)
Mg_2Si/Al–Si^{54}	K_2TiF_6	~100 μm	~ 30 μm at (3 wt% of K_2TiF_6)
Mg + 5Si/Mg–Si^{24}	KBF_4 + K_2TiF_6 ratio (4 : 1)	~100 μm	~20 μm at (5 wt% of KBF_4 + K_2TiF_6)
Mg_2Si/Al–Si–Cu^{55}	Cerium	~100 μm	~15 μm at (0.4 wt% Ce)
Al–Mg_2Si^{56}	Lithium	~30 μm	~15 μm at (0.3 wt% of lithium)
Mg–4%Si alloy[57]	Strontium	~46 μm	~16 μm at 3% Al–10% Sr

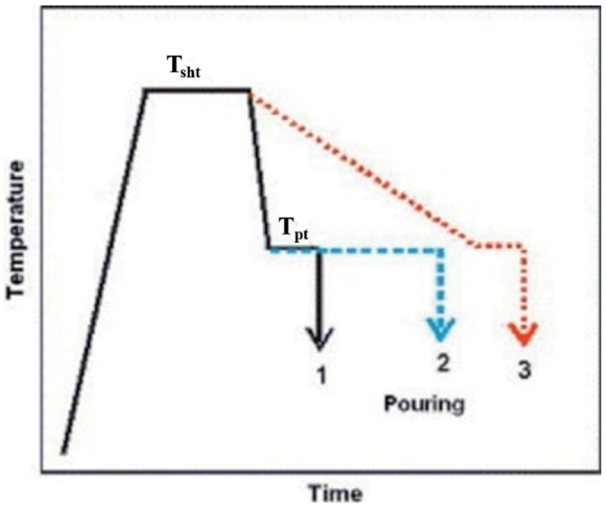

Fig. 8 Schematic of typical superheating process with three different temperature profiles. This figure has been reproduced from ref. 58 with permission from Elsevier, copyright 2007.

for the primary Mg_2Si phase particles. Therefore, the growth of Mg_2Si particles is significantly influenced. On the addition of yttrium (0.1 or 0.4 wt%), the average grain size of primary and eutectic Mg_2Si phase particles is not significantly reduced. However, the addition of 0.8 wt% of yttrium reduces the average grain size of primary Mg_2Si phase particles from 100 μm to ~30 μm. The average grain size of the primary Mg_2Si phase increases with the increase in wt% of yttrium (Fig. 6).

Wang *et al.*[24] modified the Mg–5 wt% Si alloy with K_2TiF_6, KBF_4 and $KBF_4 + K_2TiF_6$. The unmodified microstructure of Mg–5 wt% Si alloy consists of coarse primary Mg_2Si crystals, Chinese script eutectic Mg_2Si phase particles, and α-Mg. The average grain size of the Mg_2Si phase in the unmodified microstructure is 100 μm (Fig. 7). Table 1 shows the effect of different modifiers on the primary Mg_2Si phase, eutectic Mg_2Si phases and the grain size of the Mg_2Si phase.

Several reports are available on the modification of Mg_2Si phase particles in magnesium and aluminum alloys. A critical review of important articles concluded that bismuth and lithium show good Mg_2Si phase refinement in magnesium and aluminum alloys, respectively. Based on these reviews, Table 2 shows that the Mg_2Si phase refinement results in magnesium and aluminum alloys.

4.2 Refinement *via* superheating method

In the superheating process, the refinement of grains by applying high-temperature heating (more than 150 °C to 300 °C from the equilibrium liquidus temperature of the alloy) and holding it for a short period of time followed by rapid cooling near to the pouring temperature of the alloy melt and again holding it for a short period of time before casting. Primarily this method was reported in a British patent granted in 1931 (Fig. 8).[58]

Cao *et al.*[58] reported three different cooling conditions for Mg–Al alloys, which are shown in Fig. 8: (1) rapid cooling from T_{sht} (super heating temperature) to T_{pt} (pouring temperature) with a short holding time before casting; (2) rapid cooling from T_{sht} to T_{pt}, but with a lengthy holding time at T_{pt} before casting; and (3) slow cooling from T_{sht} to T_{pt}. In Mg–Al alloys, a high level of grain refinement requires rapid cooling of the alloy melt from T_{sht} to the pouring temperature T_{pt} and pouring it immediately (Case 1 in Fig. 8). The desirable grain refinement is achieved by the appropriate superheating temperature and time. The range of specific superheating temperatures (T_{sht}) for desirable grain refinement depends on the alloy composition.

During the last few decades extensive research has been reported and a large number of hypothesis have been proposed for various applications. The superheating process is generally used to refine the Mg_2Si phase in magnesium and aluminum alloys. Min *et al.*[59] investigated the melt superheating treatment effect on the grain refinement of Mg–3.5Si–1Al alloy as unmodified specimens or specimens modified with 0.2% Sr–Sb (mass fraction). The unmodified Mg–3.5Si–1Al alloy was refined progressively with an increase in the temperature from 750 °C to 900 °C. However, alloys modified by Sr–Sb could be refined up to a melt superheating temperature of 850 °C. A further increase in the temperature from 850 °C to 900 °C leads to a slight increase in the grain size. Gu *et al.*[60] reported that on increasing the temperature from 750 °C to 900 °C, in Mg–1.5Si–1Zn alloy, the grain size of the primary Mg_2Si phase decreased from 18 μm to 9 μm. The polyhedral morphology remains unchanged. Moreover, the grains of the eutectic Mg_2Si phase were refined without a change in morphology.

4.3 Refinement *via* rapid solidification

In the rapid solidification process the alloy melts are solidified at a high cooling rate. The cooling rate is enhanced by using substrate quenching and atomization.[61] The substrate quenching techniques include the thermal spray method, planar flow casting, the melt-spinning technique, twin rolling copper, and mold casting.[61–64] In the atomization technique the molten alloy stream of the liquid is broken into small spheres using a high-pressure jet of gas. This process includes high pressure and centrifugal gas atomization.[65] Grensing *et al.*[66] reported the microstructures of rapidly solidified magnesium–silicon alloys. Three different microstructures were observed in the rapidly solidified Mg–Si alloys: a cellular (dendritic) structure based on magnesium, a coupled eutectic structure, and a dendritic structure based on Mg_2Si. Matsuada *et al.*[67] reported that with the rapid solidification process, it is possible to produce an alloy of homogeneous composition, a fine and uniform distribution of the intermetallic phase and a highly fine-grained matrix. Mabuchi *et al.*[68] reported the tensile behavior of Mg–Mg_2Si composites processed under rapid solidification. At room temperature, the Mg–Mg_2Si composite shows an ultimate tensile strength of 506 MPa, a yield strength of 455 MPa and a percentage of elongation of 1.6% up to failure.

4.4 Refinement of Mg_2Si phase and enhancement of mechanical properties *via* mechanical working process

Mechanical working processes are the most promising approaches ensuring property enhancement in alloys and

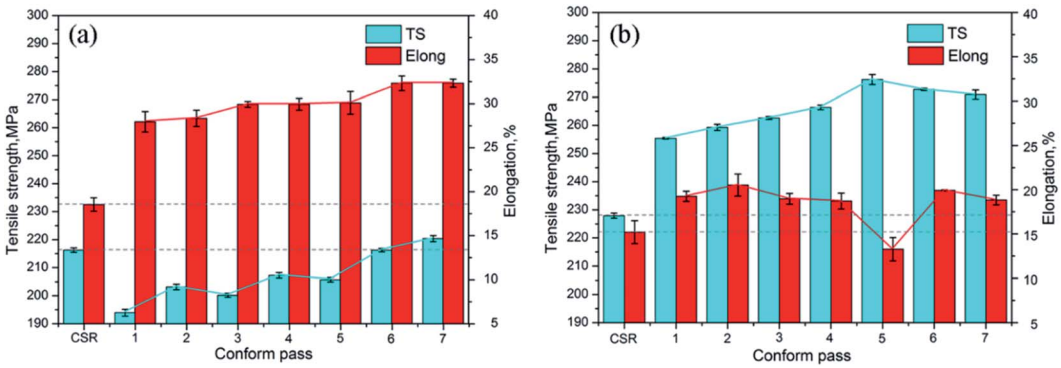

Fig. 9 The tensile strength (TS) and elongation (strain %) of the Al–Mg–Si alloy *versus* Conform pass: (a) after 1 to 7 Conform processes (N) and (b) after 1 to 7 Conform processes followed by aging at 175 °C for 8 h. This figure has been reproduced from ref. 73 with permission from Elsevier, copyright 2017.

composites.[69,70] Mechanical working processes have high potential to refine the grain and the Mg_2Si phase present in aluminum and magnesium alloys. Mabuchi *et al.*[71] synthesized Al–Mg–Si–Si_3N_4 composites with hot extrusion at 500 °C with a reduction ratio of 100 : 1. During hot extrusion, recrystallization and dynamic precipitation occurred. Therefore, very small grains, of less than 3 μm were produced. Ke *et al.*[72] reported that during the hot extrusion, dynamic recrystallization of the aluminum matrix and dynamic precipitation of deep submicron silicon and Mg_2Si particles and deformation-induced twinning of silicon particles occurred in the Al–12.0%Si–0.2% Mg alloy. By the hot extrusion process, a good combination of tensile strength and elongation (256.3 MPa and 15%, respectively) are obtained after aging for 12 hours of ESA (hot-extruded, solutionized and aged) specimens. Hu *et al.*[73] prepared Al–Mg–Si alloy with a diameter of 9.5 mm by a continuous casting and rolling process. The alloy rod was continuously deformed through the R-Conform process (repetitive continuous extrusion forming) and followed by aging at 175 °C for 8 h.

The variation in tensile properties and % of elongation (strain) of Al–Mg–Si alloys after different Conform passes with and without corresponding aging (hardening) treatment is shown in Fig. 9. The result revealed that after a single R-Conform pass, the tensile strength decreases and the percentage of elongation increases. With a further increase in the number of passes, the values of tensile strength and percentage of elongation both increase and after seven passes, the value of tensile strength is more than that of initial continuous casting and rolling (CSR) materials (from 216.2 to 220.3 MPa). After artificial aging (hardening) at 175 °C for 8 h, the tensile strength of the aged Al–Mg–Si alloys increases significantly up to a value of 276.2 MPa after artificial aging treatment after the fifth Conform pass. Moreover, on increasing the number of passes the Mg_2Si phase gradually dissolves back in the Al matrix during the initial four Conform passes, and is no longer present after the 4th Conform pass. Gazizov *et al.*[74] studied the effect of equal-channel angular pressing and aging on the microstructure and mechanical properties of Al–Cu–Mg–Si alloys. Ingots were homogenized at 500 °C for 24 h and subsequently cooled to room temperature in a furnace. Then tensile tests were performed under different conditions of equal-channel angular pressing (ECAP) and aging. The intermediate ECAP is an efficient method that allows one to increase the strength of AA 2014 alloy. After treatment (12 h aging) the yield stress ($\sigma_{0.2}$) and ultimate tensile strength (σ_{uts}) were ~415 and ~450 MPa, respectively.

4.5 Other methods

Some other methods are also available for the refinement of magnesium and aluminum alloys, such as the physical grain refinement method,[65] the agitation method,[52] the Elfinal process ($FeCl_3$),[65] carbon inoculation[52,65] and the powder metallurgy[17] process. However, in these methods insufficient reports are available for refinement of the Mg_2Si phase in magnesium and aluminum alloys. In the carbon inoculation and Elfinal processes, carbon and $FeCl_3$ are introduced into molten magnesium and aluminum alloys. The addition of carbon and $FeCl_3$ enhance heterogeneous nucleation by *in situ* precipitation in the alloy melt, forming another compound. The carbon inoculation grain refinement method is only possible in aluminum-containing magnesium alloys (normally with >2% Al).[75] Qian *et al.* reported that grain refinement of Mg–Al alloys by carbon inoculation stems from the interaction between carbon and aluminium.[75] The formation of Al_4C_3 particles provides effective nucleants for the carbon inoculation treatment. Carbon inoculation also offers many advantages, such as low operating temperature and less fading with long holding times for application in mass production.[65] Recent research indicates that the Al, C and Al_2CO particles act as effective nucleants for grain refinement of carbon inoculation. The Elfinal process involves plunging anhydrous $FeCl_3$ into melts between 740 and 780 °C. This process is effective with and without aluminum-containing magnesium alloys. This process was invented by a German magnesium company "I. G. Farbenindustrie" based on the hypothesis that iron particles could act as nucleation sites for magnesium grains. This also has a lower operating temperature than the superheating method. It provides some economic advantages and it also allows the melt to be held at the pouring temperature for at least an hour without any loss in grain

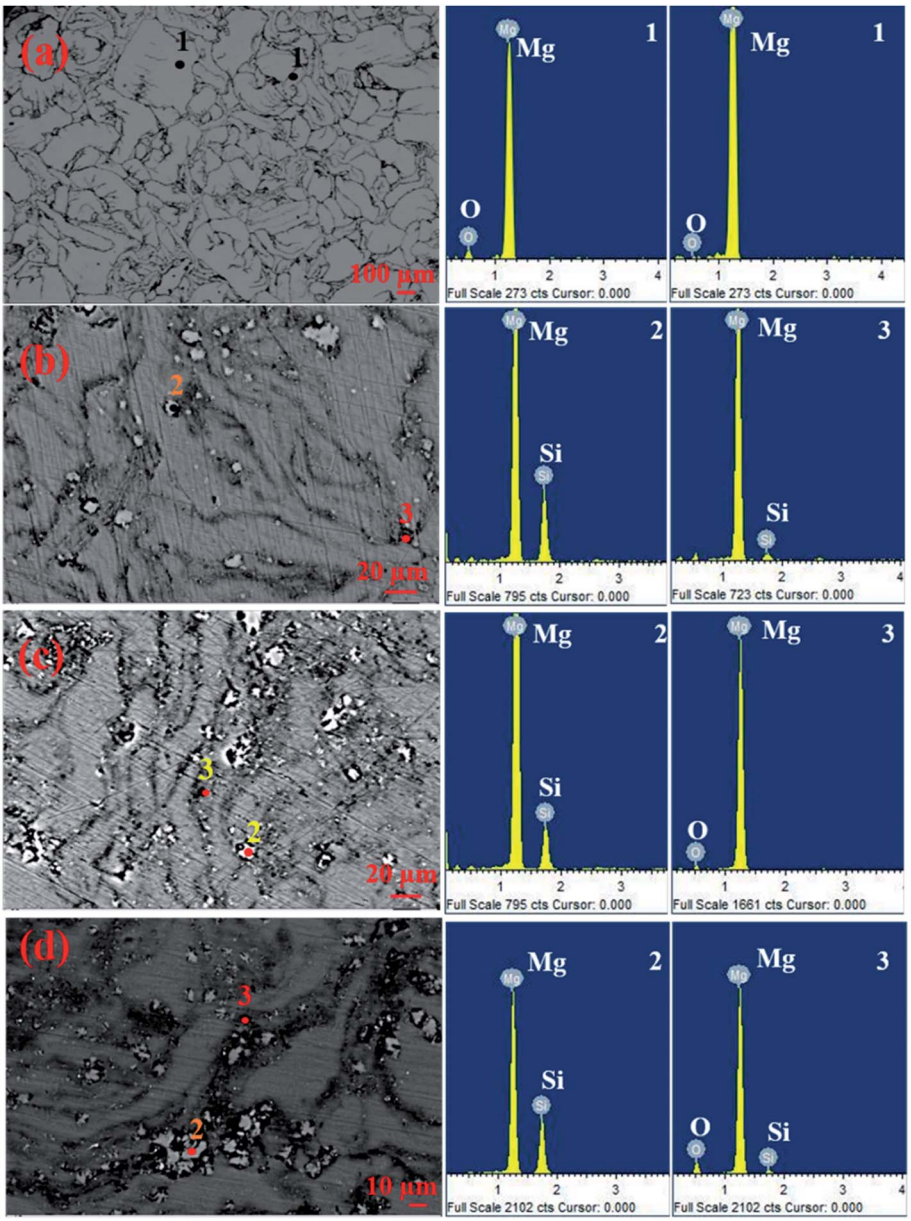

Fig. 10 (a–d) SEM micrographs with EDS spectra: (a) pure Mg, (b) Mg–1Si, (c) Mg–4Si and (d) Mg–6Si. This figure has been reproduced from ref. 17 with permission from Elsevier, copyright 2020.

refinement efficiency.[16] This method can produce a grain refining effect similar to that obtained by superheating.

Recently Seth *at el*. reported that the average grain sizes of Mg_2Si particles in Mg–1Si, Mg–4Si and Mg–6Si alloys synthesized *via* solid-state sintering using high-energy ball milling are 10 μm, 8 μm and 6 μm, respectively.[17] On increasing the amount of silicon, the average grain size of the Mg_2Si phase decreases.

Fig. 10(a–d) show the SEM and EDS spectra at different regions present in the SEM micrographs of pure Mg, Mg–1Si, Mg–4Si, and Mg–6Si alloys synthesized *via* the powder metallurgy route.[17] Each micrograph consists of three different regions: (1) matrix regions, (2) gray particles, (3) dark regions. These regions are indicated by points 1, 2 and 3, respectively. The reported results show that in each micrograph all the gray particles are present in the grain boundary and are surrounded by dark regions. The results of EDS spectral analysis at point 2 show that the Mg and Si elements are present in the gray particles. The ratio of the intensity of the spectral lines due to magnesium and silicon is equivalent to the stoichiometric ratio of magnesium and silicon in Mg_2Si. This indicates that the gray particles are the Mg_2Si phase. These results show that the formation of the Mg_2Si phase is possible using the powder metallurgy method with a finer grain size.

5. Mechanical properties

The mechanical properties of magnesium and aluminum alloys containing Mg–Si and Mg_2Si are highly satisfactory. These alloys are suitable candidates for different applications. The

Table 3 Tensile properties of Mg–Si alloy with different alloying elements

S. No	Alloy compositions	UTS (MPa)	YS (MPa)	Elongation (%)	Reference no.
1	Mg–0.6Si	166.2 ± 8	60.11 ± 2.27	6.62 ± 0.88	77
2	Mg–0.6Si–0.2Ca	154.4 ± 5.4	50.05 ± 1.13	6.62 ± 0.58	
3	Mg–0.6Si–0.4Ca	156.8 ± 4.9	56.85 ± 0.98	6.22 ± 0.24	
4	Mg–0.6Si–1.5Zn	**182.8 ± 6.3**	**53.72 ± 2.61**	**14.28 ± 0.64**	
5	Mg–0.6Si	164 ± 4	60 ± 2	6 ± 0.5	78
6	Mg–0.6Si–0.5Zn	175 ± 3	60 ± 2	13 ± 1	
7	Mg–0.6Si–1.3Zn	180 ± 2	63 ± 2	14 ± 0.5	
8	Mg–0.6Si–1.5Zn	**190 ± 2**	**62 ± 2**	**15 ± 0.6**	
9	Mg–0.6Si–1.5Zn	181 ± 2	54 ± 2	14.2 ± 1	
10	Mg	87 ± 2	—	—	79 * (T + CC: cyclic closed-die forging at 450 °C)
11	Mg ± 1.5Si	126 ± 1	—	—	
12	Mg ± 3.3 Si	85 ± 1	—	—	
13	Mg (T + CC)	126 ± 1	—	—	
14	Mg ± 1.5Si (T + CC)	132 ± 1	—	—	
15	Mg ± 3.3 Si (T + CC)	142 ± 1	—	—	

Table 4 Tensile properties of Al–Mg–Si alloys with different alloying elements

Alloy compositions	Yield strength (MPa)	Elongation (%)	Hardness (BHN)	Grain size (μm)	Reference no.
Al–0.35Mg–7Si	174.31	2.67	72.3	200–300	80
Al–0.35Mg–7Si–0.6Ba	178.51	3.76	72.3	80–150	
Al–0.35Mg–7Si–1Ba	198.04	4.06	73.5	30–80	
7Al–0.35Mg–7Si–1.4Ba	171.74	2.92	71.0	100–200	
7Al–0.35Mg–7Si–1.8Ba	167.55	2.07	70.2	—	
Al–Mg–Si longitudinal	102 ± 1	—	—	—	81
Al–Mg–Si transverse	99 ± 4	—	—	—	

Table 5 Tensile properties of Mg–Al–Si (AS series) of alloys under different conditions

Alloy compositions	Yield strength (MPa)	Elongation (%)	UTS (MPa)	Hardness (BHN)	Grain size (μm)	Reference no.
AS52 (ambient)	58 ± 3	13.75 ± 0.3	165 ± 3		—	82
AS52 (at 150 °C)	50 ± 3	15 ± 0.3	150 ± 2		—	
AS31 (ambient)	58.9	6.4	95.6	57 ± 1		83
AS31 (at 150 °C)	65.5	6.8	87.3			

specific strength and specific stiffness of materials are important for the design of lightweight components. At present, applications of high-strength lightweight components are increasing enormously in automotive and aerospace industries to save weight. Weight saving is particularly important for automotive bodies, components and other products, where energy consumption and power limitations are major concerns.[76] There are large numbers of reports available on the mechanical properties of aluminum and magnesium alloys containing the Mg_2Si phase. In general, mechanical properties are evaluated by tensile, compression and hardness tests. Some significant tensile properties of Mg–Si alloys and higher alloys containing the Mg_2Si phase are given in Tables 3–5.

5.1 Tensile properties

The yield strength of Mg–Si alloys and those with other alloying elements vary from 50 ± 1 MPa to 60 ± 1 MPa. The ultimate tensile strength (UTS), however, varies over a wider range; the Mg–0.6Si–1.5Zn alloy shows higher tensile properties.[77,78] The UTS of Mg–0.6Si, Mg–1.5Si, and Mg–3.3Si alloys are 166.2 ± 8.0 MPa, 126 ± 1 MPa and 85 ± 1 MPa, respectively. The UTS of Mg–Si alloys decreases with an increase in the silicon content. However, after secondary process (cyclic closed-die forging at 450 °C), the UTS of Mg–1.5Si and Mg–3.3Si alloys are 132 ± 1 MPa and 142 ± 1 MPa, respectively. The enhancement in UTS of Mg–1.5Si and Mg–3.3Si alloys is due to the refinement of the Mg_2Si phase during the secondary processes (Table 3).

Al–Mg–Si based aluminum alloys show better tensile properties than the Mg–Al–Si (AS series) of alloys (Table 4 and 5). The yield strength of Al–0.35Mg–7Si alloys increases on addition of alloying elements. The addition of up to 1 wt% of barium enhances the yield strength of Al–0.35Mg–7Si, as barium works as a grain modifier up to 1 wt%. The tensile properties of Al–Mg–Si also depend on the rolling direction. Test specimens cut

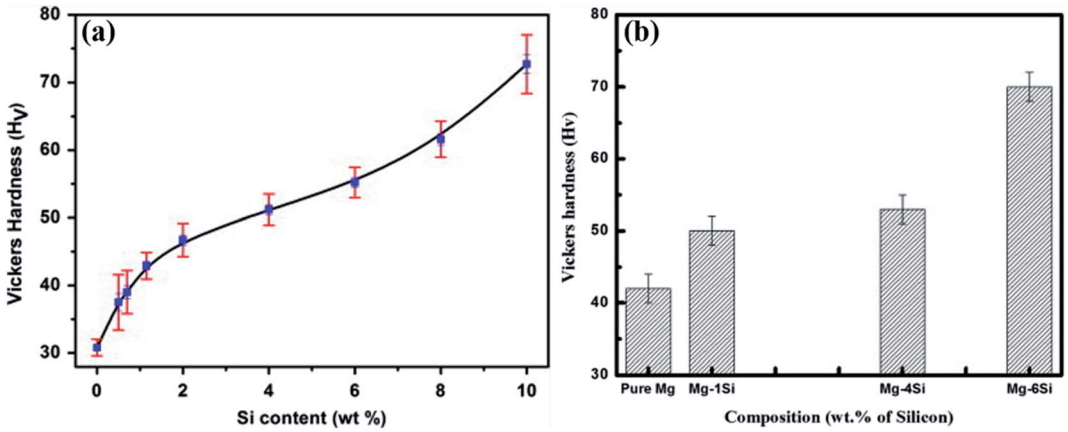

Fig. 11 Hardness behavior of Mg–Si alloys. The specimens are synthesized by: (a) casting process. This figure has been reproduced from ref. 5 with permission from Elsevier, copyright 2013. (b) Powder metallurgy process. This figure has been reproduced from ref. 17 with permission from Elsevier, copyright 2020.

Table 6 Hardness behavior of Mg–Al–Si alloys

Hardness (HV) of Mg–Al–Si (AS series) alloys[29]		
1	AS11	41 ± 1
2	AS21	48 ± 2
3	AS41	52 ± 1
4	AS61	54 ± 1
5	AS91	62 ± 1

in the longitudinal direction show better properties than specimens cut in the transverse direction in Al–Mg–Si alloys.

5.2 Hardness behavior

Fig. 11(a) and (b) show the bulk hardness behaviour of Mg–Si alloys, where the specimens are synthesised *via* the casting process (CP) and the powder metallurgy process (PM) using high-energy ball milling, respectively. The specimens prepared *via* the powder metallurgy process show higher hardness values for the same composition. The hardness values (Hv) of Mg–6Si alloys synthesized *via* the casting and powder metallurgy processes are 55 ± 2 and 72 ± 2, respectively. The specimens synthesized *via* the powder metallurgy process show smaller average grain size of the Mg_2Si phase.[17] Therefore, pinning of dislocations is greater at Mg_2Si precipitate particles in specimens synthesized *via* the powder metallurgy process. Therefore, specimens prepared by the powder metallurgy route show higher hardness values.

The addition of aluminum also improves the hardness of Mg–Si alloys. Aluminum reacts with magnesium and forms another intermetallic compound, $Mg_{17}Al_{12}$ (β-phase). The quantity of β-phase increases due to an increase in the amount of aluminum. The β-phase and Mg_2Si phase could be very effective in strengthening magnesium alloys at elevated and room temperatures.[29] Therefore, AS11 (Mg–1Al–1Si) shows lower hardness and AS91 (Mg–9Al–1Si) alloy shows higher hardness in the AS series of alloys (Table 6).

Al–Mg–Si alloys have good strength and formability. Therefore, numerous attempts have been made to improve the strength and ductility of these alloys while maintaining their formability. Artificial aging is the one of the best methods to improve the strength and ductility of these alloys.[84] Generally artificial aging was done on heat-treatable (Al–Mg–Si) alloys. During the artificial aging process, the supersaturated solid solution present in alloys decomposes into fine precipitates that strengthen the alloys by acting as obstacles to the movement of dislocations. The nano-scale dispersive precipitates increase both the strength and the ductility of the alloys.[85] Hu *et al.*[84] reported the Vickers microhardness of Al–Mg–Si alloys with nano-scale precipitates after repetitive continuous extrusion forming (R-Conform passes) and T8 tempering (aging at 120, 155 and 175 °C for various times up to 8 h). Table 7 shows the results of the maximum micro-hardness value with respect to

Table 7 Maximum Vickers micro-hardness values of Al–Mg–Si alloys with respect to aging time of four different mechanical working conditions.[84]

	Maximum micro-hardness with respect to aging time			
Aging temperatures	Direct drawing	1R-Conform passes and drawing	4R-Conform passes and drawing	7R-Conform passes and drawing
RT	92.5 ± 0.2	91.5 ± 0.2	106 ± 0.2	109 ± 0.2
120 °C	95.2 ± 0.2 (2 h)	103 ± 1 (1 h)	108 ± 0.4 (3 h)	112 ± 0.5 (3 h)
155 °C	93 ± 0.4 (2 h)	96.5 ± 0.5 (1 h)	105 ± 0.2 (3 h)	107 ± 0.2 (2 h)
175 °C	85 ± 0.6 (1 h)	96 ± 0.3 (2 h)	96.5 ± 0.4 (1 h)	97 ± 0.5 (1 h)

aging time of four different conditions: direct drawing, 1R-Conform passes and drawing, 4R-Conform passes and drawing, and 7R-Conform passes and drawing. All specimens are aged at 120, 155 and 175 °C for various durations up to 8 hours (1 hour intervals).

The results of Table 7 reveal that the hardness of specimens with and without aging increased with increasing number of R-Conform passes. The specimens aged at 120 °C show higher hardness values under all conditions. The specimens with 7R-Conform passes and drawing and aged at 120 °C for 3 hours show maximum micro-hardness values among all the specimens.

The hardness behavior and other mechanical properties of Mg–Si, Mg–Si–Al and Al–Mg–Si alloys are due to the precipitation behavior and decomposition of a supersaturated solid solution of fine particles during the synthesis process, secondary mechanical working (severe plastic deformation, cold and hot extrusion) processes and artificial aging under different conditions (temperatures and holding time).

Mg–Si, Mg–Si–Al and Al–Mg–Si alloys show a wide range of mechanical properties. Therefore, they have the ability to be used in different applications according to the properties required. Generally Mg–Si and Mg–Si–Al alloys are used for manufacturing components which are used in high-temperature applications (higher creep resistance).[86] The formability of Al–Mg–Si alloys is high. Therefore, these alloys are used to form sheets and wires. The applications of these alloys are briefly explained in the next section.

6. Applications based on properties

Magnesium and aluminum alloys containing an Mg_2Si phase cover a wide area of applications. Generally, magnesium-based alloys (Mg–Si and Mg–Si–Al) are used in automotive, aerospace, biomedical, and electronics applications. However, aluminum-based alloys (Al–Mg–Si) are used in automotive, aerospace and, electrical applications. These alloys have a variety of miscellaneous advantageous properties: *e.g.* light weight, high specific strength, good castability, low elastic modulus, recyclability, high corrosion resistance, thermal stability, low thermal conductivity, higher electrical conductivity, and low toxicity.[87] Based on these properties, Mg–Si and Mg–Si–Al alloys are heavily used in biomedical applications for transplantation into human bones and teeth. Moreover, these alloys are used in automotive and aerospace applications for body and engine components which are working at high temperature. These alloys are also used in electronic applications.[88] Al–Mg–Si alloys are used for making single-shape relatively complex architectural forms and body-cover parts of automobiles and aerospace vehicles. These alloys have the ability to withstand maximum tensile and compressive stresses. This characteristic is particularly important for structural components where stiffness is critically important. These alloys are also used in electrical applications for wire manufacturing.

6.1 Application of magnesium alloys containing an Mg_2Si phase

Mg–Si and Mg–Si–Al alloys have outstanding characteristics, including higher creep resistances, excellent damping performance, high stiffness–weight ratio and they are highly biocompatible for the human body. Due to their mechanical properties and biocompatibility, these alloys are heavily used in biomedical applications. Aluminum and silicon ions are also present in the human body and they are involved in many metabolic reactions and biological mechanisms. These alloys

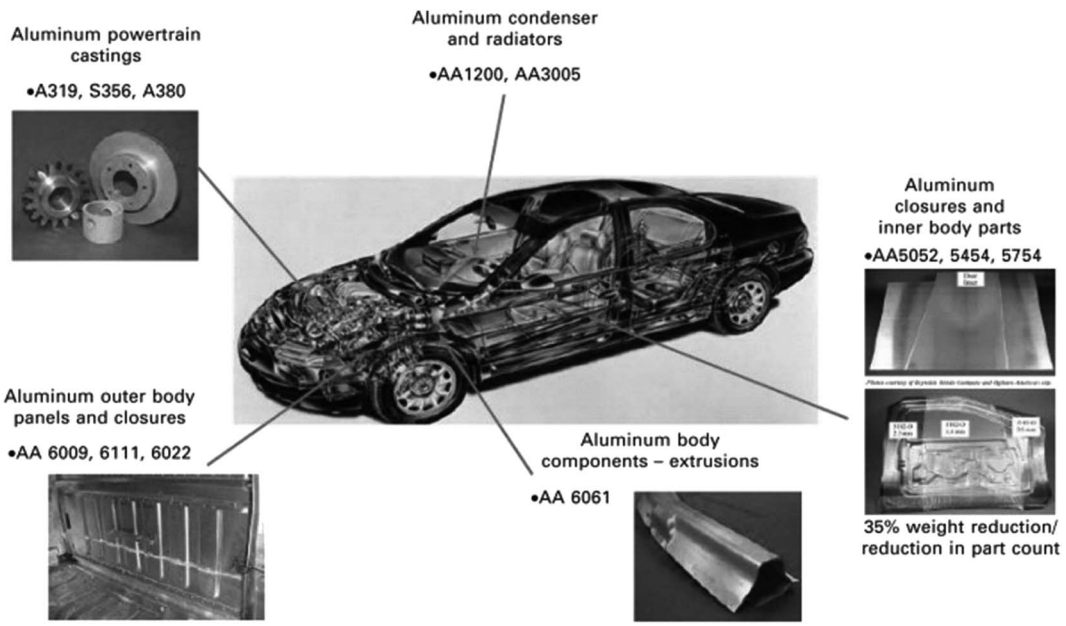

Fig. 12 Application of different series of aluminum alloys in automotive product forms. This figure has been reproduced from ref. 92 with permission from Elsevier, copyright 2010.

easily achieve similar mechanical properties to natural bone.[89] Therefore, aluminum and silicon elements are heavily used as alloying elements in magnesium alloys. These alloying elements improve the tensile strength, elongation and corrosion resistance of magnesium alloys.[90] These elements decrease the bio-degradation rate of magnesium alloys and thus can be easily optimized according to human bodily comfort. Therefore, Mg–Si and Mg–Si–Al alloys are heavily used in biomedical applications. Magnesium alloys containing the Mg_2Si phase are heavily used as structural materials, especially in the automotive and aerospace industries. Due to their low density and good mechanical properties, these alloys have received interest for being more economical for fuel consumption due to a reduction in weight and SOX, NOX, and CO_2 emissions.[29] These alloys are used for the manufacturing of crank cases for air-cooled automobile engines, and for the production of clutch pistons and blade stators.[91]

6.2 Application of aluminum alloys containing an Mg_2Si phase

Aluminum alloys containing an Mg_2Si phase are heavily used in aerospace, marine, automotive, and smart phone cases applications. Only the 6XXX series of alloys definitely contain magnesium and silicon. These alloys are used to form complex architectural shapes because they have the unique feature of great extrudability.[92] Engler *et al.*[32] reported that the 6XXX series of alloys are used to manufacture sheets for automobile body panel applications to enhance fuel efficiency and reduce vehicle emissions:[93] *e.g.* AA6009, AA6010, AA6016, AA6111 and AA6181A alloys. The automotive body panel components, including platform frame rails and cross members, seat frames, space frames, radiator frames and bumper beams, are manufactured using these alloys. The extruded aluminum alloy (6000 series) is also used in bus and heavy truck components in drive shafts, transmission parts, air intake manifolds, sun roofs, and air bag modules. Kolobnev *et al.*[94] reported an Al–0.3Mg–0.5Si alloy with a low (0.5–0.8%) content of copper to enhance its hardness upon artificial aging at 180 °C. Moreover, this alloy can be used for a long time (4300 h) at 90 °C (for example, in an automobile radiator).

Fig. 12 shows the application of different series of aluminum alloys in automotive product forms. The AA6009, AA6111, AA6022 and AA6061 alloys are used in outer body panels and closures. These alloys are commonly used in external body panels due to the resistance of these alloys to "ludering" or strain marking in stamping and their higher strength. Murashkin *et al.*[33] reported that Al–Mg–Si alloys, such as 6101 and 6201, are widely used to produce electrical and power conductors for self-supporting insulated lines and overhead power transmission lines. These alloys are used to form wires of various diameters with a yield strength of 275–330 MPa.

7. Summary

The present review has focused on studies of Mg–Si, Mg–Si–Al, and Al–Mg–Si lightweight higher alloys containing an Mg_2Si phase along with several grain refinement methods and their mechanical properties. It has been found that the mechanical properties of magnesium and aluminum alloys containing an Mg_2Si phase depend on the average grain size, morphology, synthesis process, and secondary processes. In Mg–5Si alloys, Ba (bismuth) shows the highest grain refinement ability compared to other grain modifiers. On 0.5 wt% addition of bismuth, Mg–5Si alloy shows a minimum average grain size of 15 μm. The secondary processes also help in the refinement of the Mg_2Si phase. In Al–Mg–Si alloys, the Mg_2Si phase gradually dissolves back into the Al matrix during R-Conform passes and artificial aging at 175 °C for 8 h.[73] The carbon inoculation grain refinement method is not applicable for Mg–Si alloys. This method only works in the presence of aluminum in magnesium and aluminum alloys. The Elfinal and carbon inoculation processes work in a lower temperature range compared to the superheating method. To the best of our knowledge, no reports are available on the refinement of the Mg_2Si phase *via* the Elfinal and carbon inoculation processes. The formation of a fine Mg_2Si phase is also possible by the powder metallurgy method using high-energy ball milling. The average grain sizes of the Mg_2Si phase in Mg–1Si, M–4Si and Mg–6Si alloys are 10 μm, 8 μm and 6 μm, respectively. An increase in the wt% of silicon decreases the average grain size of the Mg_2Si phase.[17] Specimens with a finer Mg_2Si phase show a high hardness value, larger wear resistance, high specific strength, and creep resistance. Lightweight high-strength Mg–Si, Mg–Si–Al and Al–Mg–Si alloys are being successfully used in the automotive and aerospace industries for weight saving of body and engine components to enhance energy saving. Scope for high-level research is available for the synthesis process, phase modification and evolution of mechanical properties of magnesium and silicon alloys containing the Mg_2Si phase.

Conflicts of interest

There are no conflicts to declare.

Acknowledgements

One of the authors, Mr Prem Prakash, acknowledges the Indian Institute of Technology (Banaras Hindu University) Varanasi for proving funds as financial support.

References

1 S. Tekumalla, S. Seetharaman, A. Almajid and M. Gupta, Mechanical Properties of Magnesium-Rare Earth Alloy Systems: A Review, *Metals*, 2015, **5**, 1–39.
2 H. Z. Ye and X. Y. Liu, Review of recent studies in magnesium matrix composites, *J. Mater. Sci.*, 2004, **39**, 6153–6171.
3 B. L. Mordike and T. Ebert, Magnesium Properties — applications — potential, *Mater. Sci. Eng., A*, 2001, **302**, 37–45.
4 Y. Sun, C. Li, Y. Liu, L. Yu and H. Li, Intermetallic phase evolution and strengthening effect in Al–Mg_2Si alloys with different Cu/Ni ratios, *Mater. Lett.*, 2018, **215**, 254–258.

5 K. K. A. Kumar, U. T. S. Pillai, B. C. Pai and M. Chakraborty, Dry sliding wear behaviour of Mg–Si alloys, *Wear*, 2013, **303**, 56–64.
6 G. B. Hamu, D. Eliezer and K. S. Shin, The role of Mg_2Si on the corrosion behavior of wrought Mg–Zn–Mn alloy, *Intermetallics*, 2008, **16**, 860–867.
7 B. E. Sawe, *The Most Abundant Elements In the Earth's Crust*, World Atlas, 2018.
8 S. M. T. I. Nayim, M. Z. Hasan, P. P. Seth, P. Gupta, S. Thakur, D. Kumar and A. Jamwal, Effect of CNT and TiC hybrid reinforcement on the micro-mechano-tribo behaviour of aluminium matrix composites, *Mater. Today: Proc.*, 2020, **21**, 1421–1424.
9 S. Hossain, M. M. Rahman, D. Chawla, A. Kumar, P. P. Seth, P. Gupta, D. Kumar, R. Agrawal and A. Jamwal, Fabrication, microstructural and mechanical behavior of Al-Al_2O_3-SiC hybrid metal matrix composites, *Mater. Today: Proc.*, 2020, **21**, 1458–1461.
10 M. Gupta and W. L. E. Wong, Magnesium-based nanocomposites: Lightweight materials of the future, *Mater. Charact.*, 2015, **105**, 30–46.
11 E. J. Guo, B. X. Ma and L. P. Wang, Modification of Mg_2Si morphology in Mg–Si alloys with Bi, *J. Mater. Process. Technol.*, 2008, **206**, 161–166.
12 Q. C. Jiang, H. Y. Wang, Y. Wang, B. X. Ma and J. G. Wang, Modification of Mg_2Si in Mg–Si alloys with yttrium, *Mater. Sci. Eng., A*, 2005, **392**, 130–135.
13 H. Y. Wang, W. Wang, M. Zha, N. Zheng, Z. H. Gu, D. Li and Q. C. Jiang, Influence of the amount of KBF_4 on the morphology of Mg_2Si in Mg–5Si alloys, *Mater. Chem. Phys.*, 2008, **108**, 353–358.
14 W. Liping, G. Erjun and M. Baxia, Modification effect of lanthanum on primary phase Mg_2Si in Mg-Si alloys, *J. Rare Earths*, 2008, **26**, 105–109.
15 Z. H. Gu, H. Y. Wang, N. Zheng, M. Zha, L. L. Jiang, W. Wang and Q. C. Jiang, Effect of melt superheating treatment on the cast microstructure of Mg–1.5Si–1Zn alloy, *J. Mater. Sci.*, 2008, **43**, 980–984.
16 Y. C. Lee, A. K. Dahle and D. H. StJOHN, The Role of Solute in Grain Refinement of Magnesium, *Metall. Mater. Trans. A*, 2000, **31**, 2895–2906.
17 P. P. Seth, N. Singh, M. Singh, O. Prakash and D. Kumar, Formation of fine Mg_2Si phase in Mg-Si alloy *via* solid-state sintering using high energy ball milling, *J. Alloys Compd.*, 2020, **821**(153205), 1–10.
18 K. Kondoh, H. Oginuma, R. Tuzuki and T. Aizawa, Magnesium matrix composite with solid-state synthesized Mg_2Si dispersoids, *Mater. Trans.*, 2003, **44**(4), 611–618.
19 K. Kondoh, H. Oginuma, A. Kimura, S. Matsukawa and T. Aizawa, In-situ Synthesis of Mg_2Si Intermetallics *via* Powder Metallurgy Process, *Mater. Trans.*, 2003, **44**(5), 981–985.
20 X. Zhu, H. Yang, X. Dong and S. Ji, The effects of varying Mg and Si levels on the microstructural inhomogeneity and eutectic Mg_2Si morphology in die-cast Al–Mg–Si alloys, *J. Mater. Sci.*, 2019, **54**, 5773–5787.
21 X. Zhou, T. Guo, S. Wu, S. Lu, X. Yang and W. Guo, Effects of Si Content and Ca Addition on Thermal Conductivity of As-Cast Mg–Si Alloys, *Materials*, 2018, **11**(2376), 1–12.
22 Y. Pan, X. Liu and H. Yang, Microstructural formation in a hypereutectic Mg–Si alloy, *Mater. Charact.*, 2005, **55**, 241–247.
23 L. Chen, H. Y. Wang, Y. J. Li, M. Zha and Q. C. Jiang, Morphology and size control of octahedral and cubic primary Mg_2Si in an Mg–Si system by regulating Sr contents, *CrystEngComm*, 2014, **16**, 448–454.
24 H. Y. Wang, Q. C. Jiang, B. X. Ma, Y. Wang, J. G. Wang and J. B. Li, Modification of Mg_2Si in Mg–Si alloys with K_2TiF_6, KBF_4 and KBF_4 + K_2TiF_6, *J. Alloys Compd.*, 2005, **387**, 105–108.
25 G. R. Ma, X. L. Li, L. Xiao and Q. F. Li, Effect of holding temperature on microstructure of an AS91 alloy during semisolid isothermal heat treatment, *J. Alloys Compd.*, 2010, **496**, 577–581.
26 B. Bronfin, M. Katsir and E. Aghion, Preparation and solidification features of AS21 magnesium alloy, *J. Mater. Sci. Eng. A*, 2001, **302**, 46–50.
27 S. Candan and E. Candan, A comparative study on corrosion of Mg−Al−Si alloys, *Trans. Nonferrous Met. Soc. China*, 2017, **27**, 1725–1734.
28 P. Zhang, Creep behavior of the die-cast Mg–Al alloy AS21, *Scr. Mater.*, 2005, **52**, 277–282.
29 B. Akyuz, Wear and machinability properties of AS series magnesium alloys, *J. Eng. Manuf.*, 2016, **230**(4), 701–709.
30 K. Bandil, H. Vashisth, S. Kumar, L. Verma, A. Jamwal, D. Kumar, N. Singh, K. K. Sadasivuni and P. Gupta, Microstructural, mechanical and corrosion behaviour of Al–Si alloy reinforced with SiC metal, *J. Compos. Mater.*, 2019, 1–9.
31 S. Ji, W. Yang, F. Gao, D. Watson and Z. Fan, Effect of iron on the microstructure and mechanical property of Al–Mg–Si–Mn and Al–Mg–Si die cast alloys, *J. Mater. Sci. Eng. A*, 2013, **564**, 130–139.
32 O. Engler and J. Hirsch, Texture control by thermo-mechanical processing of AA6xxx Al – Mg – Si sheet alloys for automotive applications — a review, *Mater. Sci. Eng., A*, 2002, **336**, 249–262.
33 M. Murashkin, A. Medvedev, V. Kazykhanov, A. Krokhin, G. Raab, N. Enikeev and R. Z. Valiev, Enhanced Mechanical Properties and Electrical Conductivity in Ultrafine-Grained Al 6101 Alloy Processed *via* ECAP-Conform, *Metals*, 2015, **5**, 2148–2164.
34 K. C. H. Kumar, N. Chakraborti, H. L. Lukas, O. Bodak and L. Rokhlin, *Aluminium – Magnesium – Silicon*, MSIT, Landolt-Bornstein New Series, vol. IV/11A3, pp. 165–177.
35 W. Yang, M. Wang, R. Zhang, Q. Zhanga and X. Sheng, The diffraction patterns from β'' precipitates in 12 orientations in Al–Mg–Si alloy, *Scr. Mater.*, 2010, **62**, 705–708.
36 A. K. Gupta, D. J. Lloyd and S. A. Court, Precipitation hardening in Al–Mg–Si alloys with and without excess Si, *Mater. Sci. Eng., A*, 2001, **316**, 11–17.
37 A. Mandal and M. M. Makhlouf, Chemical modification of morphology of Mg_2Si phase in hypereutectic aluminum–

silicon– magnesium alloys, *Int. J. Cast Met. Res.*, 2010, **23**(5), 303–309.

38 S. J. Andersen, C. D. Marioara, A. Frøseth, R. Vissers and H. W. Zandbergen, Crystal structure of the orthorhombic U2-$Al_4Mg_4Si_4$ precipitate in the Al–Mg–Si alloy system and its relation to the and phases, *J. Mater. Sci. Eng. A*, 2005, **390**, 127–138.

39 A. Kumar, S. Kumar and N. K. Mukhopadhyay, Introduction to magnesium alloy processing technology and development of low-cost stir casting process for magnesium alloy and its composites, *J. Magnesium Alloys*, 2018, **6**, 245–254.

40 E. Aghion and B. Bronfin, Magnesium alloys deployment towards the 21th Century, *Mater. Sci. Forum*, 2000, **350–351**, 19–30.

41 M. S. Dargusch, A. L. Bowles, K. Pettersen, P. Bakke and G. L. Dunlop, The effect of silicon content on the microstructure and creep behavior in die-cast magnesium AS alloys, *Metall. Mater. Trans. A*, 2004, **35**, 1905–1909.

42 D. K. Dwivedi, R. Sharma and A. Kumar, Influence of silicon content and heat treatment parameters on mechanical properties of cast Al–Si–Mg alloys, *Int. J. Cast Met. Res.*, 2006, **19**(5), 275–282.

43 A. Jamwal, P. P. Seth, D. Kumar, R. Agrawal, K. K. Sadasivuni and P. Gupta, Microstructural, tribological and compression behaviour of copper matrix reinforced with Graphite-SiC hybrid composites, *Mater. Chem. Phys.*, 2020, **251**, 1–8.

44 A. Jamwal, P. Prakash, D. Kumar, N. Singh, K. K Sadasivuni, K. Harshit, S. Gupta and P. Gupta, Microstructure, wear and corrosion characteristics of Cu matrix reinforced SiC–graphite hybrid composites, *J. Compos. Mater.*, 2019, 1–9.

45 W. Brian James, Powder Metallurgy Methods and Applications, *ASM Handbook, Powder Metallurgy*, 2015, 7, pp. 9–19.

46 M. Scharrer, A. Lohmüller, R. M. Hilbinger, H. Eibisch, R. Jenning, M. Hartmann, R. F. Singer , Advances in magnesium injection molding (thixomolding), *Proceedings of the 7th International Conference Magnesium Alloys and Their Applications*, Dresden,Wiley VCH, 2006, pp. 248–255.

47 B. Sun, S. Li, H. Imai, J. Umeda and K. Kondoh, Synthesis kinetics of Mg2Si and solid-state formation of Mg–Mg2Si composite, *Powder Technol.*, 2012, **217**, 157–162.

48 C. Suryanarayana, *Mechanical Alloying: A Novel Technique to Synthesize Advanced Materials*, 2019, pp. 1–17.

49 X. Niu, Formation of Magnesium Silicide by Mechanical Alloying, *Adv. Perform. Mater.*, 1997, **3**, 275–283.

50 J. Jung and I. H. Kim, Synthesis of thermoelectric Mg_2Si by mechanical alloying, *J. Korean Phys. Soc.*, 2010, **574**, 1005–1009.

51 T. Aizawa and R. Song, Mechanically induced reaction for solid-state synthesis of Mg_2Si and Mg_2Sn, *Intermetallics*, 2006, **14**, 382–391.

52 E. Karakulak, A review: past, present and future of grain refining of magnesium castings, *J. Magne. Alloy.*, 2019, **7**, 355–369.

53 H. C. Shin, J. Son, B. K. Min, Y. S. Choi, K. M. Cho, D. H. Cho and I. M. Park, The effect of Ce on the modification of Mg_2Si phases of as-cast eutectic Mg-Si alloys, *J. Alloys Compd.*, 2019, **792**, 59–68.

54 Y. G. Zhao, Q. D. Qin, Y. Q. Zhao, Y. H. Liang and Q. C. Jiang, In situ Mg_2Si/Al–Si composite modified by K2TiF6, *Mater. Lett.*, 2004, **58**, 2192–2194.

55 Y. G. Zhao, Q. D. Qin, W. Zhou and Y. H. Liang, Microstructure of the Ce-modified *in situ* Mg_2Si/Al–Si–Cu composite, *J. Alloys Compd.*, 2005, **389**, L1–L4.

56 R. Hadian, M. Emamy and J. Campbell, Modification of Cast Al-Mg_2Si Metal Matrix Composite by Li, *Metall. Mater. Trans. B*, 2009, **40B**, 822–832.

57 T. S. Qiu, Z. J. Xue, T. C. Wen and Y. Y. Sheng, Morphology modification of Mg_2Si by Sr addition in Mg-4%Si alloy, *Trans. Nonferrous Met. Soc. China*, 2011, **21**, 1932–1936.

58 P. Cao, M. Qianb and D. H. StJohn, Mechanism for grain refinement of magnesium alloys by superheating, *Scr. Mater.*, 2007, **56**, 633–636.

59 Z. Min, W. H. yuan, L. Bo, Z. Bing, L. M. li, L. Dong and J. Qichuan, Influence of melt superheating on microstructures of Mg-3.5Si-1Al alloys, *Trans. Nonferrous Met. Soc. China*, 2008, **18**, s107–s112.

60 Z. H. Gu, H. Y. Wang, N. Zheng, M. Zha, L. L. Jiang, W. Wang and Q. C. Jiang, Effect of melt superheating treatment on the cast microstructure of Mg–1.5Si–1Zn alloy, *J. Mater. Sci.*, 2008, **43**, 980–984.

61 L. A. Jacobson and J. Mckittrick, Rapid solidification processing, *Mater. Sci. Eng.*, 1994, **R 11**, 355–408.

62 Govind, K. S. Nair, M. C. Mittal, K. Lal, R. K. Mahant and C. S. Sivaramakrishnan, Development of rapidly solidified (RS) magnesium–aluminium–zinc alloy, *J. Mater. Sci. Eng. A*, 2001, **304–306**, 520–523.

63 J. Cai, G. C. Ma, Z. Liu, H. F. Zhang and Z. Q. Hu, Influence of rapid solidification on the microstructure ofAZ91HP alloy, *J. Alloys Compd.*, 2006, **422**, 92–96.

64 H. Watari, T. Haga, N. Koga and K. Davey, Feasibility study of twin roll casting process for magnesium alloys, *J. Mater. Process. Technol.*, 2007, **192–193**, 300–305.

65 S. Changjiang, H. Qingyou and Z. Qijie, *Review of grain refinement methods for as-cast microstructure of magnesium alloy*,China Foundry, 2009, pp. 93–103.

66 F. C. Grensing and H. L. Fraser, Structure and Properties of Rapidly Solidified Magnesium-Silicon Alloys, *Mater. Sci. Eng.*, 1988, **98**, 313–319.

67 A. Matsuda, C. C. Wan, J. M. Yang and W. H. Kao, Rapid Solidification Processing of a Mg-Li-Si-Ag Alloy, *Metall. Mater. Trans. A*, 1996, **27A**, 1363–1370.

68 M. Mabuchi, K. Kubota and K. Higash, High strenJ. Magnesium Alloysgth and high strain rate super-plasticity in a Mg-Mg_2Si composite, *Scr. Metall. Mater.*, 1995, **33**(2), 331–335.

69 P. P. Seth, A. Das, H. N. Bar, S. Sivaprasad, A. Basu and K. Dutta, Evolution of dislocation density during tensile deformation of BH-220 steel at different pre-strain conditions, *J. Mater. Eng. Perform.*, 2015, **24**, 2779–2783.

70 U. J. P. Kumar, P. Gupta, A. K. Jha and D. Kumar, Closed die deformation behavior of cylindrical iron–alumina metal

matrix composites during cold sinter forging, *J. Inst. Eng. (India): Ser. D*, 2016, **97**(2), 135–151.

71 M. Mabuchi, H. Iwasaki, K. Higashi and T. G. Langdon, Processing and superplastic properties of fine grained Si_3N_4/AI-Mg-Si composites, *J. Mater. Sci. Technol.*, 1995, **11**, 1295–1299.

72 D. Ke, L. Hengcheng, J. Qiumin and T. Yun, Effect of hot extrusion on mechanical properties and microstructure of near eutectic Al–12.0% Si–0.2% Mg alloy, *J. Mater. Sci. Eng. A*, 2010, **527**, 6887–6892.

73 J. Hu, J. Teng, X. Ji, D. Fu, W. Zhang and H. Zhang, Enhanced mechanical properties of an Al-Mg-Si alloy by repetitive continuous extrusion forming process and subsequent aging treatment, *J. Mater. Sci. Eng. A*, 2017, **695**, 35–44.

74 M. R. Gazizov, A. V. Dubina, D. A. Zhemchuzhnikova and R. O. Kaibyshev, Effect of Equal Channel Angular Pressing and Aging on the Microstructure and Mechanical Properties of an Al–Cu–Mg–Si Alloy, *Phys. Met. Metallogr.*, 2015, **116**(7), 718–729.

75 Ma Qian and P. Cao, Discussions on grain refinement of magnesium alloys by carbon inoculation, *Scripta Mater.*, 2005, **52**, 415–419.

76 M. K. Kulekci, Magnesium and its alloys applications in automotive industry, *Int. J. Adv. Manuf. Technol.*, 2008, **39**, 851–865.

77 E. Zhang, L. Yang, J. Xu and H. Chen, Microstructure, mechanical properties and bio-corrosion properties of Mg–Si(–Ca, Zn) alloy for biomedical application, *Acta Biomater.*, 2010, **6**, 1756–1762.

78 E. Zhang, X. Wei, L. Yang, J. Xu and C. Song, Effect of Zn on the microstructure and mechanical properties of Mg–Si alloy, *J. Mater. Sci. Eng. A*, 2010, **527**, 3195–3199.

79 J. Metayer, B. Ye, W. Guo, Q. Wang, H. Zhou and F. Mollet, Microstructure and mechanical properties of Mg_2Si alloys processed by cyclic closed-die forging, *Trans. Nonferrous Met. Soc. China*, 2014, **24**, 66–75.

80 X. H. Zhang, G. C. Su, C. W. Ju, W. C. Wang and W. L. Yan, Effect of modification treatment on the microstructure and mechanical properties of Al–0.35%Mg–7.0%Si cast alloy, *Mater. Des.*, 2010, **31**, 4408–4413.

81 O. V. Panchenko, L. A. Zhabrev, D. V. Kurushkin and A. A. Popovich, Macrostructure and Mechanical Properties of Al – Si, Al – Mg – Si, AND Al – Mg – Mn Aluminum Alloys Produced by Electric Arc Additive Growth, *Met. Sci. Heat Treat.*, 2019, **60**(11 – 12), 749–754.

82 B. H. Kim, S. W. Lee, Y. H. Park and I. Park, The microstructure, tensile properties, and creep behavior of AZ91, AS52 and TAS652 alloy, *J. Alloys Compd.*, 2010, **493**, 502–506.

83 B. Wang, X. Wang, J. Zhou, G. Zhang and F. Liu, Effects of solution heat treatment on microstructure and mechanical properties of Mg–3Al–1Si–0.3Mn–xSr alloy, *J. Mater. Sci. Eng. A*, 2014, **618**, 210–218.

84 J. Hu, W. Zhang, D. Fu, J. Teng and H. Zhang, Improvement of the mechanical properties of Al–Mg–Si alloys with nano-scale precipitates aftern repetitive continuous extrusion forming and T8 tempering, *J. Mater. Res. Technol.*, 2019, **8**(6), 5950–5960.

85 J. P. Hou, Q. Wang, Z. J. Zhang, Y. Z. Tian, X. M. Wu, H. J. Yang, X. W. Li and Z. F. Zhang, Nano-scale precipitates: The key to high strength and high conductivity in Al alloy wire, *Mater. Des.*, 2017, **132**, 148–157.

86 M. Govindaraju, U. Chakkingal, P. R. Kalvala, R. V. Vignesh and K. Balasubramanian, Investigations on the Creep behavior of friction-stir-processed magnesium alloy AE42, *J. Mater. Eng. Perform.*, 2020, **29**, 3172–3182.

87 D. Vojtěch, H. Čížovál and K. Volenec, Investigation of magnesium-based alloys for biomedical applications, *Kovove Mater.*, 2006, **44**, 211–223.

88 H. Y. Wang, L. Chen, B. Liu, X. R. Li, J. G. Wang and Q. C. Jiang, Heterogeneous nucleation of Mg_2Si on $Sr_{11}Sb_{10}$ nucleus in Mg-x(3.5, 5 wt.%) Si-1Al alloys, *Mater. Chem. Phys.*, 2012, **135**, 358–364.

89 G. E. J. Poinern, S. Brundavanam and D. Fawcett, Biomedical Magnesium Alloys: A Review of Material Properties, Surface Modifications and Potential as a Biodegradable Orthopedic Implant, *Am. J. Biomed. Eng.*, 2012, **2**(6), 218–240.

90 N. Li and Y. Zheng, Novel Magnesium Alloys Developed for Biomedical Application: A Review, *J. Mater. Sci. Technol.*, 2013, **29**(6), 489–502.

91 L. Čížek, A. Hanus , O. Blahož, T. Tański, L. A. Dobrzański, M. Praźmowski, and L. Pawlica, *Structure and mechanical properties of Mg-Si alloys at elevated temperatures*, 2009, vol. 35, pp. 37–46.

92 C. Benedyk, *Materials, Design and Manufacturing for Lightweight Vehicles*, Woodhead Publishing Limited, 2010, pp. 79–113.

93 Z. Xu, H. Ma, N. Zhao and Z. Hu, Investigation on compressive formability and microstructure evolution of 6082-T6 aluminum alloy, *Metals*, 2020, **10**, 1–11.

94 N. I. Kolobnev, L. B. Ber, L. B. Khokhlatova and D. K. Ryabov, Structure, properties and application of alloys of the Al – Mg – Si – (Cu) system, *Met. Sci. Heat Treat.*, 2012, **53**, 440–444.